NeuroImage: Clinical 41 (2024) 103575

Contents lists available at ScienceDirect

NeuroImage: Clinical

journal homepage: www.elsevier.com/locate/ynicl

Lesion mapping and functional characterization of hemiplegic children with different patterns of hand manipulation

Antonino Errante [a,b,1], Francesca Bozzetti [a,b,1], Alessandro Piras [a], Laura Beccani [c], Mariacristina Filippi [c], Stefania Costi [c,d], Adriano Ferrari [c,d], Leonardo Fogassi [a,*]

[a] Department of Medicine and Surgery, University of Parma, Parma, Italy
[b] Department of Diagnostics, Neuroradiology Unit, University Hospital of Parma, Parma, Italy
[c] Unità per le gravi disabilità dell'età evolutiva, Azienda USL—IRCCS di Reggio Emilia, Reggio Emilia, Italy
[d] Department of Surgery, Medicine, Dentistry and Morphological Sciences, University of Modena and Reggio Emilia, Modena, Italy

ARTICLE INFO

Keywords:
Cerebral palsy
Lesion classification
Voxel-based morphometry
Upper limb
Action execution
Functional reorganization

ABSTRACT

Brain damage in children with unilateral cerebral palsy (UCP) affects motor function, with varying severity, making it difficult the performance of daily actions. Recently, qualitative and semi-quantitative methods have been developed for lesion classification, but studies on mild to moderate hand impairment are lacking. The present study aimed to characterize lesion topography and preserved brain areas in UCP children with specific patterns of hand manipulation. A homogeneous sample of 16 UCP children, aged 9 to 14 years, was enrolled in the study. Motor assessment included the characterization of the specific pattern of hand manipulation, by means of unimanual and bimanual measures (Kinematic Hand Classification, KHC; Manual Ability Classification System, MACS; House Functional Classification System, HFCS; Melbourne Unilateral Upper Limb Assessment, MUUL; Assisting Hand Assessment, AHA). The MRI morphological study included multiple methods: (a) qualitative lesion classification, (b) semi-quantitative classification (sq-MRI), (c) voxel-based morphometry comparing UCP and typically developed children (VBM-DARTEL), and (d) quantitative brain tissue segmentation (q-BTS). In addition, functional MRI was used to assess spared functional activations and cluster lateralization in the ipsilesional and contralesional hemispheres of UCP children during the execution of simple movements and grasping actions with the more affected hand. Lesions most frequently involved the periventricular white matter, corpus callosum, posterior limb of the internal capsule, thalamus, basal ganglia and brainstem. VMB-DARTEL analysis allowed to detect mainly white matter lesions. Both sq-MRI classification and q-BTS identified lesions of thalamus, brainstem, and basal ganglia. In particular, UCP patients with *synergic* hand pattern showed larger involvement of subcortical structures, as compared to those with *semi-functional* hand. Furthermore, sparing of gray matter in basal ganglia and thalamus was positively correlated with MUUL and AHA scores. Concerning white matter, q-BTS revealed a larger damage of fronto-striatal connections in patients with *synergic* hand, as compared to those with *semi-functional* hand. The volume of these connections was correlated to unimanual function (MUUL score). The fMRI results showed that all patients, but one, including those with cortical lesions, had activation in ipsilesional areas, regardless of lesion timing. Children with *synergic* hand showed more lateralized activation in the ipsilesional hemisphere both during grasping and simple movements, while children with *semi-functional* hand exhibited more bilateral activation during grasping. The study demonstrates that lesion localization, rather than lesion type based on the timing of their occurrence, is more associated with the functional level of hand manipulation. Overall, the preservation of subcortical structures and white matter can predict a better functional outcome. Future studies integrating different techniques (structural and functional imaging, TMS) could provide further evidence on the relation between brain reorganization and specific pattern of manipulation in UCP children.

Abbreviations: AHA, Assisting Hand Assessment; CP, cerebral palsy; HFCS, House Functional Classification System; KHC, kinematic hand classification; MACS, Manual Ability Classification System; MUUL, Melbourne Unilateral Upper Limb assessment; UCP, unilateral cerebral palsy.

* Corresponding author.
E-mail address: leonardo.fogassi@unipr.it (L. Fogassi).

[1] These authors equally contributed to this work.

https://doi.org/10.1016/j.nicl.2024.103575
Received 2 October 2023; Received in revised form 22 January 2024; Accepted 7 February 2024
Available online 10 February 2024

1. Introduction

During typical development, the ability to reach and grasp objects represents one of the most important skills to acquire, even in the early stages of life. In the case of brain damages occurring during early development, such as those typically occurring in children with cerebral palsy (CP), the ability to control and coordinate arm/hand movements can be disrupted, making it difficult to perform daily activities (Krägeloh-Mann & Cans, 2009). CP is "a group of permanent disorders of movement and posture that are attributed to non-progressive disturbances occurring in the developing or infant brain" (Rosenbaum et al., 2007). In addition to motor impairments, CP often involves problems with sensation, perception, cognition, communication, behavior, or epilepsy and secondary musculoskeletal problems. It is the most common cause of physical disability in children, affecting approximately 2 out of 1000 live births (Oskoui et al., 2013; Sellier et al., 2016), with about 36 % of cases being unilateral CP (UCP) (Smithers-Sheedy et al., 2016), where one side of the body is more affected.

The upper limb deficits observed in these children are described with a significant range of clinical variations (Klingels et al., 2012; Sakzewski et al., 2010). In fact, while some children show subtle deficits, others have strong impairments, for example do no execute adequate reaching and grasping movements. This variability can be attributed, in principle, to diverse neurodevelopmental factors, including timing, location and extent of the underlying brain lesion (Ferrari & Cioni, 2010).

Regarding specific localization and etiopathogenetic pattern of brain lesions occurring in the immature brain (Krägeloh-Mann, 2004; Krägeloh-Mann & Cans, 2009; Krägeloh-Mann & Horber, 2007) the categorization is typically based on predominant pattern of damage, including: (a) *cortical maldevelopments*, occurring during the first 24 weeks of gestation and found in approximately 16 % of UCP cases; (b) *periventricular white matter* (PWM) lesions, commonly observed in preterm children, develop between 24 and 34 weeks of gestation and present in around 36 % of UCP children; (c) *cortical and deep gray matter* (CDGM) lesions, affecting cortical and subcortical areas, mostly occurring between 34 weeks of gestation and 28 days after birth, accounting for 31 % of UCP cases. Lesions that do not fit into these categories are usually classified as miscellaneous, comprising 7 % of UCP children. Additionally, 10 % of brain scans appear normal (Korzeniewski et al., 2008; Krägeloh-Mann & Cans, 2009; Robinson et al., 2009).

Concerning the relation between lesion and hand function, PWM lesions are associated with better hand function and less movement pathology compared to late-onset CDGM lesions. Interestingly, the integrity of the basal ganglia and/or thalamus is crucial for developing good motor function (Crichton et al., 2020; Feys et al., 2010; Holmefur et al., 2013; Holmström et al., 2010). Generally, smaller lesions lead to better functional outcomes (Fiori et al., 2015; Holmström et al., 2010; Staudt et al., 2002, 2004). However, individual factors alone cannot explain the existing variability. Overall, the literature suggests that lesion location and extent have a stronger impact on upper limb motor function in children with CDGM lesions compared to PWM lesions (Mailleux et al., 2017).

In 1999, Cioni and colleagues proposed another classification system that categorizes lesions according to the timing of their occurrence (Cioni et al., 1999). This classification, based on 91 hemiplegic children, provides valuable insights into the relationship between the timing of brain damage and the resulting motor impairments, subdividing brain lesions into four main groups. Each lesion group corresponds to a different severity of motor impairments frequently observed in individuals with UCP:

Type I: *Early malformative lesions* (1st and 2nd trimester), characterized by brain malformations, often complex, especially related to early migration disorders. Hand impairments in these patients are moderate to severe, and the prognosis appeared to be quite unfavorable as far as motor function and epilepsy were concerned.

Type II: *Prenatal lesions* (3rd trimester), such as hemorrhage of the periventricular white matter, or periventricular leukomalacia. Hand impairments in prenatal lesions are often mild or moderate and may involve spasticity, involuntary movements, and difficulties in fine motor control.

Type III: *Perinatal lesions* occurring at term and primarily characterized by acute insults to the brain, often resulting in hypoxic-ischemic injuries; sometimes the lesion affects the deeper branches with involvement of diencephalic structures (especially the posterior limb of the internal capsule and thalamus), and putamen, especially in dyskinetic forms; hand impairments are typically severe, presenting spasticity, contractures, and difficulties in grasping and fine motor skills.

Type IV: *Early acquired lesions* occurring after the perinatal period and caused by traumatic brain injuries, infections, or other acquired conditions; hand impairments vary depending on the location and extent of the lesion but commonly involve difficulties in fine motor control, coordination, and dexterity.

Although there is some evidence indicating the importance of these neurodevelopmental factors, to date, a common observation is the lack of a direct relationship between lesions and specific functional outcome in terms of hand function in individuals with UCP (Franki et al., 2020). Studies are needed that combine different methodologies of analysis (Weinstein et al., 2018), including structural analyses based on imaging techniques, to make quantitative investigations of lesions and spared areas, and functional MRI (fMRI) investigations, based on different motor tasks. Task-based fMRI has primarily been employed in UCP to investigate alterations in functional connectivity patterns in the brain (Gaberova et al., 2018). These studies have revealed that the functional network of the motor system can exhibit contralateral, ipsilateral, or bilateral activation when patients use the more affected hand, depending on the underlying mechanisms of brain reorganization (Guzzetta et al., 2007; Staudt et al., 2002). However, no studies are available about functional activations and laterality of the activated clusters in UCP children in relation to specific patterns of hand manipulation, in particular those with moderate impairment.

Significant progress has been made in the last decade, both in terms of structural characterization of lesions and functional analysis of manipulation patterns. In 2015, Fiori and colleagues (Stella Maris group, Pisa, Italy) developed a semi-quantitative scale for the classification of brain lesions observed in UCP children (Fiori et al., 2014, 2015). The scale is designed to assess both the primary lesion and abnormalities of subcortical structures that may contribute to functional impairments. Furthermore, the scale is helpful in identifying patterns and associations between lesion features and clinical manifestations, contributing to improve prognostic assessments and treatment strategies. To date, the scale has predominantly been employed for assessing PWM lesions rather than CDGM lesions (Fiori et al., 2015). Furthermore, the studies conducted thus far using this scale have involved a heterogeneous UCP population, often including children with severe deficits (Pagnozzi et al., 2020; Tinelli et al., 2020). Unfortunately, dedicated research examining the influence of lesion timing, extent, and localization in children with mild or moderate impairments in hand manipulation is missing.

A recent classification of manipulation patterns, proposed by Ferrari and Cioni (Ferrari & Cioni, 2010), enables a more precise description of the specific impairments in hand function of UCP children, useful for example to recruit selected samples of patients involved in fMRI studies (Errante et al., 2019), and helps to guide personalized intervention strategies to improve their manipulation skills (Verzelloni et al., 2021). The main purpose of the present study was to characterize, by using combined structural MRI methods, the specific lesion pattern and the preserved brain areas in children with UCP showing specific mild and moderate patterns of hand manipulation, described as "semi-functional" and "synergic" patterns. A second aim was to describe brain activations

in the same patients, by using two fMRI motor paradigms with different complexity, to determine whether the lateralization of brain activation in UCP children changes depending on the employed task.

2. Materials and methods

2.1. Study design and analysis pipeline

The study consists in a cross-sectional investigation based on MRI and behavioral data collected in a selected cohort of children with UCP (see inclusion criteria). Motor assessment included the characterization of the specific pattern of manipulation, by means of unimanual and bimanual measures (Fig. 1). The MRI based investigation included both morphological methods, to investigate lesion patterns, and functional methods based on the execution of simple movements and grasping actions, to assess spared functional activations and cluster lateralization in the ipsilesional and contralesional hemispheres. The study was approved by the local ethics committee (Comitato Etico Area Vasta Emilia Nord – AVEN) and was conducted in accordance with The Code of Ethics of the World Medical Association (Declaration of Helsinki). Parental written informed consent for all participants was obtained.

2.2. Patients

Children with UCP were selected by the special Unit for Children Rehabilitation of the UDGEE, (AUSL-IRCCS Reggio Emilia, Italy), from September 2019 to September 2022, starting from a large sample of 74 UCP patients. The inclusion criteria were: (1) confirmed diagnosis of spastic UCP (according to MRI and clinical history) (Bax et al., 2005); (2) predominant spasticity rather than dystonia or weakness interfering with upper limb function according to the definition of motor type (Sanger et al., 2003); (3) age 9 to 14 years at time of recruitment; (4) mild or moderate upper limb disability, that is, active use of affected upper limb ranging from poor active assisted use to spontaneous use, according to House Functional Classification System (HFCS) (House et al., 1981; Koman et al., 2008) with grades between 4 and 7. These HFCS levels correspond to *semi-functional hand* or *synergic hand* by Ferrari and Cioni's Kinematic Hand Classification (Ferrari and Cioni, 2010) (see paragraph 2.3, and Suppl. Table 1 for a complete description of the two patterns of hand manipulation); (5) sufficient collaboration and comprehension to participate to the MRI investigation.

Children were excluded based on the following criteria: (1) presence of sensory impairments, especially visual deficits of central origin; (2) history of seizures or seizures well controlled by therapy; (3) surgery of the more affected upper limb within 8 months prior to the recruitment; (4) BoNT-A injections to the more affected upper limb within 6 months prior to the recruitment; (5) presence of metal implants, shunts, and so on, unsuitable for execution of MRI exams; (6) severe cognitive disability, controlled by Raven's Progressive Colored Matrices (CPM) (Pueyo et al., 2008).

2.3. Assessment of unimanual and bimanual ability

All patients enrolled in the study were classified according to the HFCS for assessing upper limb function. HFCS consists of nine grades ranging from a completely excluded hand (grade 0) to a spontaneous

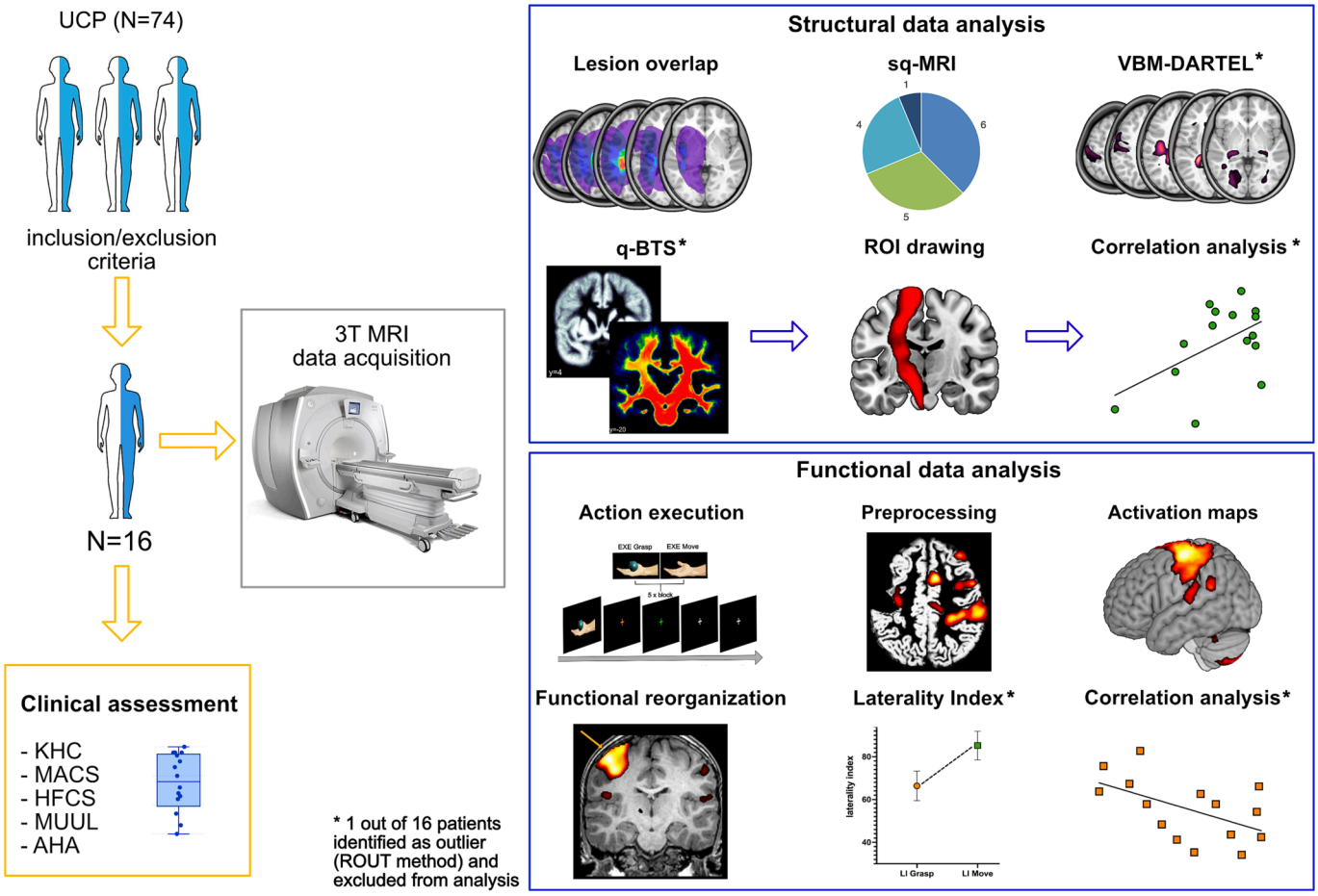

Fig. 1. Overview of the study pipeline. AHA = Assisting Hand Assessment; HFCS = House Functional Classification System; KHC = Kinematic Hand Classification; MACS = Manual Ability Classification System; MUUL = Melbourne Unilateral Upper Limb assessment; q-BTS = quantitative Brain Tissue Segmentation; sq-MRI = semi-quantitative MRI-based classification; VBM = voxel-based morphometry.

and independent one (grade 8) (House et al., 1981). In addition, they were clinically assessed with two standardized functional tests, Assisting Hand Assessment (AHA, Version 4.4) (Holmefur et al., 2007) and Melbourne Assessment of Unilateral Upper Limb Function (MUUL) (Randall et al., 2014), in order to evaluate assisting hand use during bimanual performance and upper limb movement capacity, respectively. The AHA is administered through a semi-structured play session, which requires bimanual handling and lasts 15 min. Video scoring produces raw values ranging from 22 (low ability) to 88 (high ability) that are converted in units (Louwers et al., 2017). AHA was administered and scored by a certified rater. MUUL is a standardized tool for measuring quality of upper limb movement capacity during 16 criterion-referenced items representative of reach, grasp, release, and manipulation. Performance is videotaped and scored using criteria for rating qualities of movement range, fluency, and dexterity. Scores vary from 0 to 100 %, the latter indicating best performance. Presence or absence of mirror movements in the unaffected hand during voluntary unimanual movements of the affected hand was evaluated by consensus of two experienced child physical therapists, analyzing the videotapes of the standardized clinical tests. Forms of walking were described according with the classification of walking proposed by Ferrari and Cioni (2010) (see Suppl. Table 2).

Besides these clinical measures, a specific classification of UCP children was performed according to five patterns of manipulation, by analyzing hand kinematic profile and functional use (Ferrari & Cioni, 2010). Based on Kinematic Hand Classification (KHC), children participating in this study use their non-preferred upper limb by means of *semi-functional* or *synergic* manipulation strategies:

- *semi-functional hand* is characterized by the presence of a terminolateral pinch with substantially adduced thumb. Orientation, anticipation and pre-adaptation of the hand are possible, but uncertain. The object can be promptly passed from one hand to the other, but its release is rough, with frequent need of visual control. This pattern shows, during bimanual activities, a good cooperation between the two hands. The non-preferred hand is used spontaneously as first only when the patient acts in the extreme part of the hemispace ipsilateral to this hand.
- *synergic hand* is characterized by a stereotyped grasping showing flexion and extension synergies and servomotor movements in the releasing action. The object is passed with difficulties from the non-preferred hand to the preferred one, with necessity of visual control. Manipulation is extremely limited. In this pattern, there can be a collaboration in bimanual activities for achieving the same aim, with the non-preferred hand supporting the preferred one.

A more complete description of the main features of *synergic* and *semi-functional* manipulation patterns is reported in Suppl. Table 1.

2.4. MRI data acquisition

MR images were acquired with a 3 T General Electric scanner (MR750 Discovery) equipped with a 32-channel receiver head-coil. A 3D isotropic T1-weighted-images sequence was acquired with the following parameters: 196 slices, 280 × 280 matrix with a spatial resolution of 1 × 1 × 1 mm, TR = 9700 ms, TE = 4 ms, FOV = 252 × 252 mm; flip angle = 9°. Functional volumes were acquired during motor task, with the following parameters: forty axial slices of functional images covering the whole brain acquired using a gradient-echo echo-planar imaging (EPI) pulse sequence, slice thickness = 3 mm, plus interslice gap = 0.5 mm, 64 × 64 × 37 matrix with a spatial resolution of 3.5 × 3.5 × 3.5 mm, TR = 2000 ms, TE = 30 ms, FOV = 205 × 205 mm^2, flip angle = 90°, in plane resolution = 3.2 × 3.2 mm^2.

2.5. Lesion topography

Using the unique T1-weighed images, all lesions were analyzed through two different methods including (a) qualitative lesion classification, (b) semi-quantitative classification (sq-MRI), (c) voxel-based morphometry (VBM-DARTEL), and (d) quantitative brain tissue segmentation (q-BTS) (Fig. 1).

2.5.1. Lesion mapping and qualitative classification

Lesion location was identified on MRI scans registered to the Montreal Neurological Institute (MNI) space for pediatric data (age 4.5 to 18.5 years) (Fonov et al., 2011). Lesions drawing was performed blindly and independently by a certified expert neuroradiologist (FB), using MRIcron software (ch2better; https://www.nitrc.org/projects/mricron). Note that structural images of children with right hemisphere lesions (left UCP) were flipped in the right-left direction (using SPM Image Calculator toolbox), in order to have all lesioned hemispheres (ipsilesional, IL) on the left side of the standard brain and all unaffected hemispheres (contralesional, CL) on the right side.

Lesions were classified through a qualitative descriptive method, starting from the involvement of the gray matter (cortical) and the white matter. In particular, the degree of white matter loss, and consequently of ventricular dilatation, was classified as mild, moderate, or severe based on the involvement of subcortical, periventricular, and deep white matter. The degree of corpus callosum atrophy was classified as mild (1), moderate (2), severe (3), based on the extent of its involvement. Ventricle dilatation was classified as minimal, mild, moderate or severe, based on the extent of its involvement. Signs of Wallerian degeneration of the cortico-spinal tract and presence of hemispheric cerebellar atrophy were also reported. Lastly, considering the different archetypes of childhood hemiplegia, the lesions were characterized using the classification proposed by Cioni et al. (1999).

2.5.2. Semi-quantitative lesion classification

Lesions were classified according to the method proposed by Fiori and colleagues, consisting in a semi-quantitative classification (sq-classification) (Fiori et al., 2014, 2015). As first step, individual lesions were manually mapped by an expert neuroradiologist delineating the boundary of the lesion directly on six axial slices, selected from the T1 Montreal Neurological Institute (MNI) template CH2. The six slices were chosen from equidistant axial images with z-values of 58, 42, 28, 12, −2, and −16. In a second step, raw scores for each lobe, subcortical structures (basal ganglia, thalamus, posterior limb of the internal capsule, and brainstem), corpus callosum and cerebellum were calculated. The scoring procedure results in summary scores for right and left hemisphere: lobar score (frontal, parietal, temporal, occipital, bilateral maximum score of 6 for each lobe); hemispheric score (which summarize frontal, parietal, temporal and occipital scores, up to bilateral maximum score of 24); subcortical score (which results from the sum of lenticular, caudate, posterior limb of the internal capsule, thalamus, and brainstem scores, up to a bilateral maximum score of 10); global score (summary score of both hemispheres plus corpus callosum and cerebellum scores, maximum score of 40). In this classification, higher score represents more severe pathology.

2.5.3. VBM-DARTEL analysis

Maps of white and gray matter of UCP patients were compared by using Voxel Based Morphometry (VBM) with that of a control group of children with typical development (TD, N = 57, 22 females and 35 males, age range from 6 to 14 years, mean age 9.3 ± 2.8 years). Data about control group are available on OpenNeuro platform (Dataset ds002116). VBM has been conducted on the anatomical T1-weighted scans, using SPM12 software package (The Wellcome Centre for Human Neuroimaging, UCL; https://www.fil.ion.ucl.ac.uk/spm/) running on MATLAB R2022a (Mathworks, Natick, MA, USA). As first step, images were segmented into gray matter, white matter and cerebrospinal fluid using SPM12 standard segmentation module (Ashburner & Friston, 2005). Second, population templates (for gray and white matter) were derived from the entire image dataset using the

Diffeomorphic Anatomical Registration through Exponentiated Lie algebra (DARTEL) algorithm (Ashburner, 2007). Third, an affine registration of the DARTEL templates to the corresponding tissue probability maps in MNI space template for pediatric data (resolution 1 x 1 x 1 mm) (Fonov et al., 2011) was performed. Lastly, images were smoothed with an 8-mm full width at half maximum Gaussian kernel. After the preprocessing pipeline, the smoothed, normalized images were used for voxelwise statistical analysis (see paragraph 2.7).

2.5.4. Quantitative brain tissue segmentation (q-BTS)

To assess quantitatively the spared volume of gray and white matter in UCP patients, we performed a quantitative brain tissue segmentation (q-BTS) analysis using a Region of Interest (ROI) approach.

A first q-BTS analysis was carried out on gray matter dataset, using a set of cortical ROIs corresponding to the ipsilesional hemisphere selected from the Wake Forest University PickAtlas (WFU PickAtlas) (Maldjian et al., 2003). Cortical ROIs included four masks of cerebral cortex corresponding to: (a) Frontal lobe, (b) Parietal lobe, (c) Occipital lobe, and (d) Temporal lobe.

In order to investigate the spared volume of subcortical structures, an automated segmentation was performed using FSL-FIRST 5.0.9 (Patenaude et al., 2011), a freely available automated segmentation tool provided by the FMRIB Software Library. FSL-FIRST uses a training data-based approach combined with a Bayesian probabilistic model to determine the most probable shape of the subcortical nuclei given the intensities of the T1 image. In particular, the following structures were segmented: (a) putamen, (b) caudate nucleus, (c) thalamus, and (d) deep brainstem nuclei. A composite mask was also created including both basal ganglia, brainstem and thalamus (BG-BS-Thal mask).

A second q-BTS analysis was performed on white matter dataset, by using a set of ROIs corresponding to white matter tracts frequently damaged in hemiplegic children. Masks of specific ROI bundles were selected from BCBToolkit (https://toolkit.bcblab.com) (Foulon et al., 2018) and included: (a) corticospinal tract, (b) corpus callosum, (c) superior longitudinal fasciculus I, II, and III, (d) arcuate fasciculus, posterior, long and anterior segment, (e) fronto-striatal projections, (f) cingulum bundle. Other global masks of white matter were selected from the WFU PickAtlas and included: (a) the entire volume of white matter in the ipsilesional (IL) hemisphere, (b) the entire volume of white matter projections within the brainstem. For each patient, we extracted in each ROI the average number of gray and white matter voxels (voxel count) using the SPM Rex Toolbox (https://web.mit.edu/swg/software.htm).

2.6. fMRI motor task

After the acquisition of morphological images, UCP patients performed a motor task in which they had to execute grasping acts (*Exe Grasp*) or simple movements (*Exe Move*), using their more affected hand. The patients laid supine in the bore of the scanner in a dimly lit environment. Geometrical 3D wooden objects (sphere, cylinder, cube) were used for the task inside the MR scanner. Visual instructions were presented by means of a digital goggles system (Resonance Technology, Northridge, CA) (60 Hz refresh rate) with a resolution of 800 horizontal pixels x 600 vertical pixels with horizontal eye field of 30°. In each trial, the patient started with the paretic hand open. In *Exe Grasp*, the experimenter, present inside the MR room, gave the patient one of the three objects, according to auditory instruction provided by headphones. In *Exe Move*, the patient performed opening/closing movements with the paretic hand. Software E-Prime 2 Professional (Psychology Software Tools, Inc.; https://www.pstnet.com) was used for instruction presentation.

The task was performed in two runs, lasting about 5 min each. A mixed block/event-related paradigm was used, consisting in 16 blocks, 8 blocks for each condition. Each block included 5 motor trials, thus, in the whole experiment, the patients were required to perform 40 grasping trials and 40 simple movements trials. At the beginning of each block, an instruction cue (white drawing on a black screen) representing a hand and the type of required action/movement was presented for 2 s. During this period, the experimenter introduced the object in contact of the patient's hand. The choice of the object to be presented in each block was based on a randomized sequence. Then an orange fixation cross appeared in the center of the black screen. After 2 s, during which patients planned the grasping/movement to be executed, fixation cross color turned to green instructing the patient to perform, without vision, a series of 5 grasping trials (or 5 simple movements). The duration of each motor trial was 2 s. After each trial period, an ISI of 800 ms, in which the fixation cross became white, was presented in order to separate consecutive motor trials within the block. Thus, the duration of each execution block, including instruction, preparation and five motor trials was 18 s. Note that the analysis of the activation was focused on the execution phase (duration 14 s).

Motor blocks were interleaved with a baseline period (rest) during which the patients remained still, fixating a static white cross, presented in the middle of the screen (rest duration = 8, 10 or 12 s). The paradigm was administered alternating grasping blocks, simple movement blocks, and rest periods using a pseudorandom sequence, counterbalanced among patients.

2.7. Statistical analysis

2.7.1. Analysis of structural data

Lesion overlap was calculated by using ImageCalculator tool for SPM12 and visualized using MRIcron software. In particular, a first overlap was calculated for UCP patients with semi-functional and synergic hand, separately. An additional calculation was carried out to explore the overlap differences in patients according to their gestational age (preterm vs at term).

Linear regression analyses were performed in order to investigate possible relation between lesion severity scored with sq-MRI classification and the levels of unimanual (MUUL assessment) and bimanual (AHA scale) ability. Concerning sq-MRI scores, the ipsilesional (IL) Hemispheric score, the Global score, and the composite Subcortical score were included in the regression analysis. Differences of lesion scores between groups (*synergic* vs. *semi-functional*, and preterm vs. at term) were investigated by using Mann-Whitney non-parametric test for independent samples. P-value < 0.05 was considered to be statistically significant.

Concerning the VBM analysis, group differences in gray and white matter volumes were assessed using the general linear model (GLM) implemented in SPM12, and statistical significance was estimated from the distributional approximations of Gaussian random fields (Friston et al., 1994). Independent-sample t test was used to investigate significant differences in distribution of white and gray matter between UCP patients and TD children. Significant effects were identified using an uncorrected threshold ($p < 0.001$), followed by cluster level family-wise error (FWE) correction for multiple comparisons ($p < 0.05$).

A preliminary analysis was performed between q-BTS data obtained in TD vs. UCP patients. Statistical differences in gray/white matter voxel distribution were assessed by means of independent sample Student's t test. Then, data of q-BTS were entered in linear regression analyses, performed to investigate possible relation between number of preserved ipsilesional gray and white matter voxels in selected ROIs, and the UCP patients' level of unimanual (MUUL) and bimanual (AHA) ability. In addition, statistical differences in voxel distribution between groups (*synergic* vs. *semi-functional*, and preterm vs. at term) were investigated by using Mann-Whitney non-parametric test for independent samples. Statistical threshold set at $p < 0.05$.

2.7.2. Analysis of fMRI data

fMRI data processing was performed with SPM12. Similar to structural data, in order to combine fMRI data from UCP children in a group analysis, we designated the left hemisphere as the lesioned hemisphere

(IL), and the right hemisphere as the contralesional one (CL). The first four EPI volumes of each functional run were discarded to allow the static magnetic field to reach a steady state. For each patient, all volumes were slice-timing corrected, spatially realigned to the first volume of the first functional run and un-warped to correct for between-scan motion. Motion parameters were used as predictors of no-interest in the subsequent statistical analysis, to account for translation and rotation along the three possible dimensions as determined during the realignment procedure. The cut-off used for motion correction tolerance was the size of the voxel (3 mm). Spatial transformation derived from T1-w image segmentation was applied to the realigned EPIs for normalization and resampled in $2 \times 2 \times 2$ mm^3 voxels using trilinear interpolation in space. All functional volumes were then spatially smoothed with 6-mm full-width half-maximum isotropic Gaussian kernel (FWHM).

Statistical analysis was performed using a random-effects model, implemented in a two-level procedure. In the first-level analysis, single-subject fMRI time series were modeled using the general linear model (GLM). The design-matrix included the onsets and the durations of all events (*instruction, planning phase, Exe Grasp*, *Exe Move*) convolved with the hemodynamic response function, plus six predictors obtained from the motion correction in the realignment process to account for voxel intensity variations caused by head movement. Rest periods between blocks were considered as implicit baseline. The analysis focused on *Exe Grasp* and *Exe Move* predictors, composed by 5 consecutive trials, which were modelled as one single epoch lasting 14 s. Contrasts derived from parameter estimation were calculated. Specific effects were tested using *t*-statistical parametric maps (SPM-t), with degrees of freedom corrected for non-sphericity at each voxel.

At second-level, *t*-contrast images corresponding to *Exe Grasp* and *Exe Move* calculated in the first-level analysis were entered in a flexible ANOVA with sphericity-correction for repeated measures. In particular, we modeled two factors specifying scans and conditions, corresponding to: (a) subjects, modeling participants variability; (b) conditions, modeling task effects. Within this model, in order to investigate activations related to execution of grasping acts vs simple movements, we calculated the direct contrast between *Exe Grasp* > *Exe Move.* Statistical inference was drawn at cluster level, with a threshold of $p < 0.001$, corrected for multiple comparisons with false discovery rate (FDR) method.

Laterality index (LI) was calculated specifically for the sensorimotor cortex by comparing the size (voxel number) of homologous areas in both hemispheres. The analysis was performed using a composite mask of the sensorimotor cortex (S1/M1) selected from WFU PickAtlas. For both *Exe Grasp* and *Exe Move*, LI was obtained by computing the ratio $N_{IL} - N_{CL}/N_{IL} + N_{CL}$, where N_{CL} and N_{IL} are the number of activated voxels in the contralesional hemisphere (CL), and the ipsilesional hemisphere (IL), respectively. For hemispheric dominance, we assumed as in previous works (Sgandurra et al., 2018) a standard threshold of 0.20 in absolute value: LI > 0.20 indicates dominance in the IL hemisphere, LI < −0.20 indicates dominance in the CL hemisphere, and between 0.20 and −0.20 indicates bilateral activations.

Linear regression analyses were performed in order to investigate possible relation between LI and lesion Type according with Cioni et al. classification (1999). In addition, LI related to *Exe Grasp* and *Exe Move* were entered into linear regression analyses, to investigate possible relationship with distribution of clinical scores of unimanual and bimanual ability (MUUL/AHA). Statistical comparisons between LI during *Exe Grasp* > *Exe Move* was carried out considering the whole UCP group using Mann-Whitney test for independent samples. Concerning possible differences in LI scores between UCP patients with *semi-functional* and *synergic* hand in the two-fMRI conditions, a non-parametric ANOVA (Kruskal-Wallis rank test) was performed. Statistical inference was drawn at $p < 0.05$. As complementary analysis, in order to investigate possible laterality effects due to functional reorganization outside sensorimotor regions, we computed the LI using a whole brain approach, by selecting a left hemispheric mask corresponding to the IL hemisphere, and a right hemispheric mask corresponding to the CL hemisphere.

3. Results

Following the application of inclusion and exclusion criteria, a homogeneous sample of 16 UCP children (9 females; range 9–14 years; M = 11; SD = 1.73) was enrolled in the study, starting from an initial cohort of 74 UCP patients. Concerning gestational age, 9 children were born at term (postmenstrual age ≥37 weeks), while the remaining 7 patients were preterm, with a mean postmenstrual age of 31.4 weeks. Demographic information about the UCP groups (synergic hand, semi-functional hand) and TD control group are reported in Table 1. They were matched for age, sex, more affected side, gestational age, lesions type according with their timing, presence/absence of mirror involuntary movements, and cognitive level (Table 1). The full list of the recruited UCP patients, with individual demographic and clinical information, is reported in Suppl. Table 3. According with the KHC, 8 patients showed *synergic hand* pattern, while the remaining showed *semi-*

Table 1
Demographic and clinical characteristics of the UCP patients and control participants included in the study. Age is reported in terms of mean value ± standard deviation. The remaining values are reported as absolute numbers and percentages (in brackets). Abbreviations: CSC = Cortico-subcortical; ES = equivalent score; HFCS = House Functional Classification System; MACS = Manual Ability Classification Score; PV = periventricular; TD = Typically developed. See also Suppl. Table 1 for a description of of kinematic and functional features of synergic hand and semi-functional hand according with Kinematic Hand Classification.

	UCP Semifunctional Hand (N = 8)	UCP Synergic Hand (N = 8)	TD Controls (N = 57)	*p*-value
Age	11.1 ± 1.8	10.8 ± 1.9	9.3 ± 2.8	$P = 0.08$[a]
Sex				$P = 0.39$[b]
Males	3 (38 %)	4 (50 %)	35 (62 %)	
Females	5 (62 %)	4 (50 %)	22 (38 %)	
More affected side				$P > 0.99$[c]
Left	2 (25 %)	3 (38 %)		
Right	6 (75 %)	5 (62 %)		
Gestational Age	36.6 ± 3.4	35.1 ± 5.6		$P = 0.53$[d]
At term (=/>37 weeks)	5 (62 %)	4 (50 %)		
Preterm (<37 weeks)	3 (38 %)	4 (50 %)		
Lesion Type				$P = 0.51$[b]
Malformations (Type I)	0 (0 %)	1 (12 %)		
PV lesions (Type II)	6 (75 %)	4 (50 %)		
CSC lesions (Type III)	2 (25 %)	3 (38 %)		
MACS				*P = 0.001[b]
I-II	8 (100 %)	2 (25 %)		
III-IV	0 (0 %)	6 (75 %)		
HFCS				*P = 0.03[b]
Levels 4–5	1 (12 %)	5 (62 %)		
Levels 6–7	7 (88 %)	3 (38 %)		
Mirror movements				$P = 0.28$[c]
Present	1 (12 %)	4 (50 %)		
Absent	7 (88 %)	4 (50 %)		
Raven Matrices score				$P = 0.80$[b]
ES = 2	2 (25 %)	2 (25 %)		
ES = 3	1 (12 %)	0 (0 %)		
ES = 4	5 (63 %)	6 (75 %)		

[a] Kruskal-Wallis ANOVA.
[b] Pearson Chi-squared test
[c] Fisher exact test
[d] Student *t* test.

functional hand pattern. A description of forms of walking observed in the recruited patients is also reported (Table 1 and Suppl. Table 2).

Robust nonlinear regression with false discovery rate (FDR) method (ROUT; Motulsky and Brown, 2006) was carried out using GraphPad software, to identify possible outliers from the distribution of gray/white matter, in order to correctly interpret subsequent analyses, such as VBM, q-BTS and fMRI analyses. The results of outlier identification are reported in the Suppl. Fig. 1. The analysis (Q = 1 %) reveal that only patient 08 had an atypical distribution of gray matter and white matter volume (due to the presence of normotensive hydrocephalus), thus we excluded only this case from the subsequent analyses. In particular, patient 08 was included only in lesion overlap analysis, and sq-MRI classification, because the aim of these analyses was purely descriptive, while we excluded the outlier from any statistical comparison. No outliers were identified in TD group.

3.1. Lesion overlap and qualitative neuroradiological description

Lesions description based on qualitative neuroradiologic method is reported in Table 2. Considering the different archetypes of childhood hemiplegia, the lesions were classified as Type I (1 patient), Type II (10 patients) and Type III (5 patients) (see Table 2 and Suppl. Fig. 2). Twelve patients showed unilateral lesions, 9 in the left hemisphere and 3 in the right one. Four children had bilateral lesions with a prevalence of the hemisphere contralateral to the more affected hand. Fig. 2 shows the overlap of the most frequent lesions found in patients with semi-functional and synergic hand pattern, respectively, at cortical and subcortical level (basal ganglia, thalamus, brainstem). Note that lesions are overlaid on six axial slices corresponding to those used in sq-MRI classification. Most lesioned regions in both groups involved the periventricular (14 patients) and deep (9 patients) white matter. Six patients showed the typical periventricular (PVL) or subcortical leukomalacia as the results of insults occurred during pre- and *peri*-natal period. The lesions were characterized by white matter loss, gliosis, and cavitated/cystic lesions adjacent to the periventricular zones (secondarily dilated) or diffuse white matter injury and hypomyelination. Involvement of the cortical regions (i.e., motor, premotor and parietal cortex) was less frequently found (4 patients). One child showed associated cortical malformations (schizoencephaly and polymicrogyria). The degree of white matter loss, and consequently of ventricular dilatation (VD) was minimal in 10 patients, moderate in 5 patients, and severe in 1 patient. The degree of atrophy of the posterior sector of corpus callosum was mild in 6 patients, moderate in 4 patients, and severe in 1 patient. No patients had lesions in the anterior sector of corpus callosum. In 5 children, the corpus callosum appearance was normal. Ten patients showed signs of Wallerian degeneration of the corticospinal tract documented by secondary volumetric reduction of the ipsilesional cerebral peduncle and pons. Marginal gliosis was present in four patients, documented by slightly periventricular T1-hypointensities. For comparisons, the lesion overlap considering the group of UCP patients born preterm and at term, respectively, is shown in Suppl. Fig. 3.

3.2. Lesion analysis based on sq-MRI classification

The main results of the sq-MRI classification are shown in Fig. 3A. The average global score was 7.2 (SD = 4.3), with a range from score 1 (patient 01) to score 19 (patient 08). Six patients obtained a minimal score (comprised between 1 and 4), 5 patients obtained a mild score (between 5 and 8), 4 patients obtained a moderate score (between 9 and 12) and only 1 patient (patient 08, the same identified as outlier) obtained a severe score (above 13), presenting a large lesion due to normotensive hydrocephalus. Concerning the ipsilesional hemisphere, in most cases the lesion involved only one or two lobes (score between 1 and 6). The frontal lobe was damaged in 13 patients, the parietal lobe in 11 patients and the temporal lobe in 10 patients. Only in patient 08 the lesion also involved the occipital lobe (score > 10). Almost all the sample (with the exception of patients 01 and 07) also presented damage at the level of other regions. Of these, the most frequently affected regions were the posterior limb of the internal capsule, which was damaged in 11 patients. Atrophy of the brainstem, thalamus, and putamen was evident in 10, 9 and 6 patients, respectively. In 4 patients the lesion affected all the main regions of the ipsilesional hemisphere (score > 4). Concerning the corpus callosum, 11 patients showed lesions of the medial and/or the posterior sector, while the remaining 5 patients did not show any significant alteration.

3.3. Relation between sq-MRI scores, manipulation pattern, and other clinical measures

No significant relation was found between sq-MRI Global and IL Hemispheric score and unimanual or bimanual ability scores (Suppl. Table 4). However, more severe lesion scores in subcortical structures (Subcortical sq-MRI score) correlate with worse MUUL score ($R^2 = 0.34$; $p = 0.02$) as well as worse AHA score ($R^2 = 0.34$; $p = 0.02$) (Fig. 3B, C). Considering the hand manipulation pattern, UCP patients with synergic hand showed higher lesion Global score (Mann-Whitney U = 9, $p = 0.03$) and Subcortical score (Mann-Whitney U = 8, $p = 0.01$), as compared with UCP patients with semi-functional hand (Fig. 3D and Suppl.

Table 2
Summary of the anatomical characteristics of the lesions. The degree of white matter loss, and consequently of ventricular dilatation, was classified as mild, moderate, and severe based on the involvement of the periventricular (PV), deep (D) and subcortical (SC) white matter (WM). The degree of corticospinal tract and corpus callosum atrophy was classified as mild, moderate, severe. Abbreviations: CC = corpus callosum; CS = corticospinal tract; F = frontal lobe; GA = gestational age; GMD = gray-matter damage; HFCS = House Functional Classification System; I = insula; KHC = Kinematic Hand Classification; LH = left hemisphere; O = occipital lobe; P = parietal lobe; T = temporal lobe; VD = ventricles dilatation; WMD = white-matter damage. [a] Lesion type according with Cioni et al.'s classification (1999).

ID	Lesion Side	Lesion Type[a]	GA (wks)	GMD	WMD	PV-WM	D-WM	SC-WM	VD	Localization	CC atrophy	CS atrophy
P01	LH	III	40	xx	x	0	0	x	mild	F	normal	no
P02	LH	II	35	0	x	x	0	0	mild	P	mild	No
P03	Bilateral (RH > LH)	II	38	0	x	x	0	0	mild	P	normal	No
P04	RH	II	40	0	x	x	0	0	mild	P	normal	Yes
P05	RH	I	28	0	x	x	x	x	moderate	F-P-I	mild	Yes
P06	RH	III	41	0	x	x	x	0	moderate	F-P	moderate	Yes
P07	Bilateral (RH > LH)	II	32	0	x	x	0	0	mild	P	mild	No
P08	LH	II	36	0	x	x	x	x	severe	I-F-P-T-O	severe	Yes
P09	LH	III	40	xx	x	x	x	x	moderate	I-P	moderate	Yes
P10	LH	II	31	0	x	x	x	0	mild	F	mild	Yes
P11	Bilateral (LH > RH)	II	30	0	x	x	0	0	mild	F-P	Normal	No
P12	Bilateral (RH > LH)	II	39	0	x	x	x	0	mild	F-P	mild	Yes
P13	LH	III	37	xx	x	0	x	x	mild	I-F	moderate	Yes
P14	LH	II	39	0	x	x	x	0	moderate	F-P	moderate	Yes
P15	LH	III	28	x	x	x	x	x	moderate	I-F-P	Normal	Yes
P16	LH	II	40	0	x	x	0	0	mild	F-P	mild	No

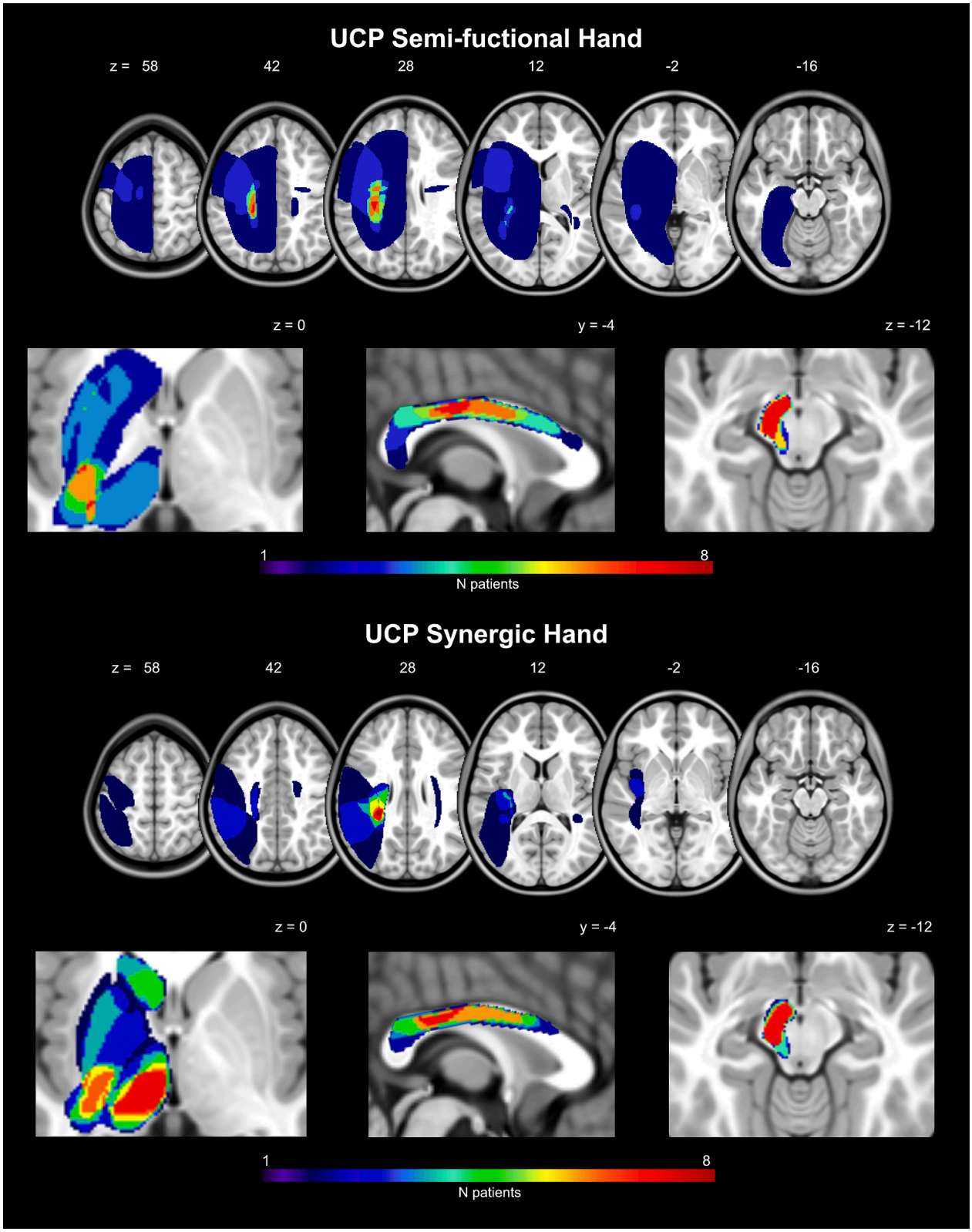

Fig. 2. Lesion overlap maps calculated separately for UCP patients with semi-functional and synergic hand, respectively, projected on a standard MNI pediatric template (Fonov et al., 2011). Maps are overlaid on the axial view of six representative slices (corresponding to those used in sq-MRI classification) and three sections at the level of basal ganglia (axial view), corpus callosum (sagittal view) and brain stem (axial view), respectively.

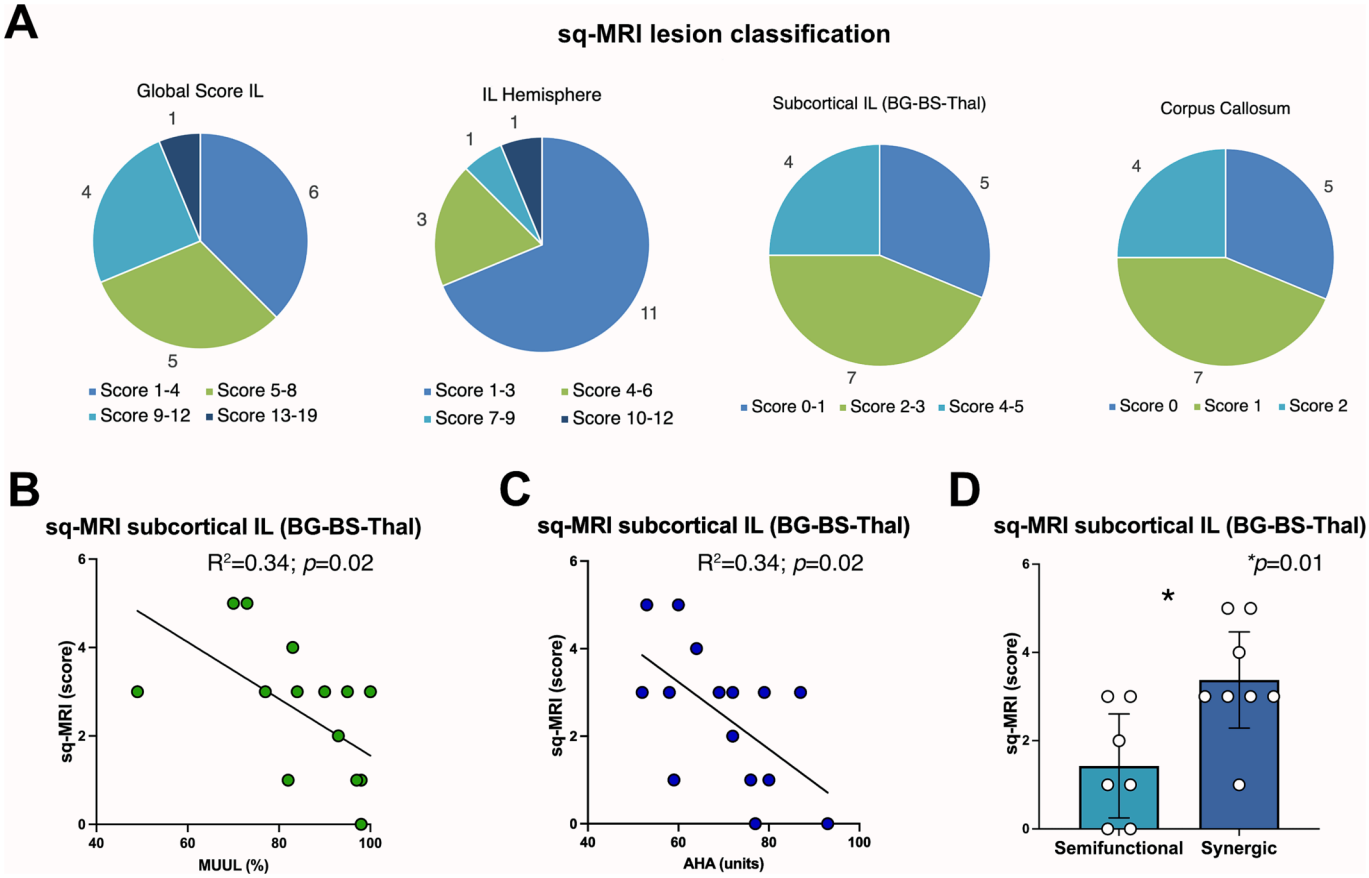

Fig. 3. Sq-mri classification results. (A) Lesion severity is reported both as global score and specific score for the ipsilesional (IL) hemisphere, IL subcortical structures, and corpus callosum. (B) Scatterplot showing the negative linear relation between MUUL score and sq-MRI subcortical score. (C) Linear negative relation between AHA score (bimanual function) and sq-MRI subcortical score. (D) Bar graph showing the difference of sq-MRI Subcortical score in patients with *synergic* and *semi-functional* hand. Error bars represent standard deviation.

Table 5). Concerning gestational age, no significant differences were present between sq-MRI lesion scores in UCP patients born at term and UCP patients born preterm (Suppl. Table 5).

3.4. Results of VBM-DARTEL analysis

The results of VBM-DARTEL analysis are presented in Fig. 4. For a visualization of individual maps of gray and white matter see Suppl.

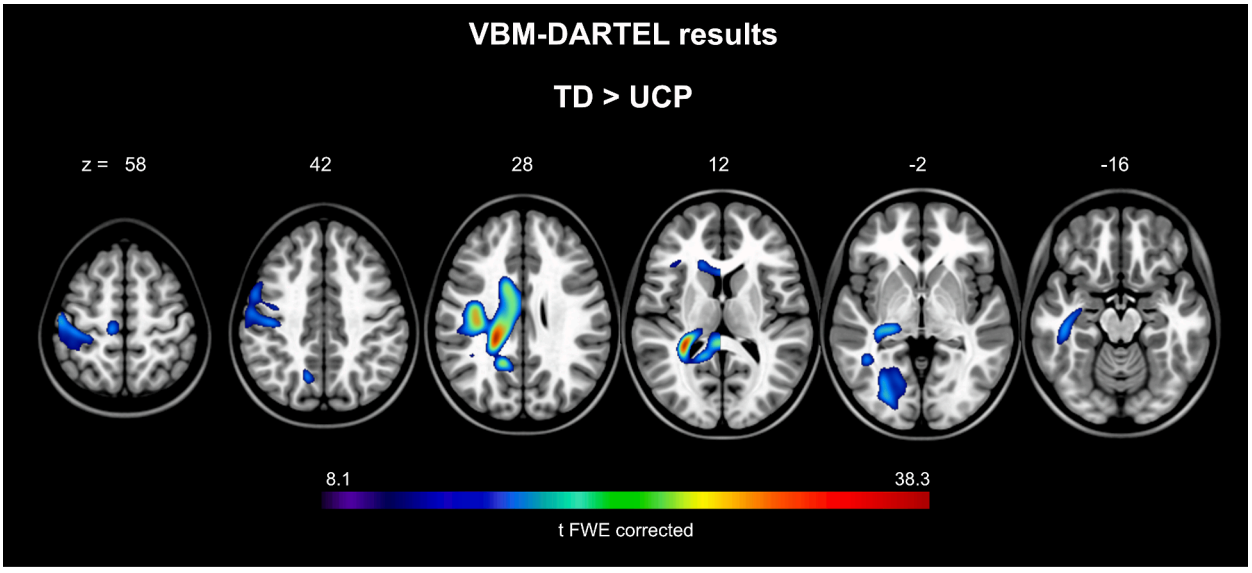

Fig. 4. VBM-DARTEL results. Differential map of the gray and white matter loss in UCP children, as compared with TD children, overlaid into six axial slices of a standard MNI pediatric template.

Figs. 4 and 5. UCP children showed statistically significant reductions in global gray and white matter volume compared with TD children ($t > 8.1$, $p = 0.05$, FWE corrected at voxel level). In particular, concerning the gray matter, UCP children showed significant reduction in the ipsilesional primary sensorimotor areas (M1/S1), premotor cortex, posterior parietal cortex and anterior insula (Fig. 4). At subcortical level, volume reduction of the thalamus was found. Concerning the white matter, as expected, UCP children exhibited significant reduction of the ipsilesional corticospinal projections, posterior limb of the internal capsule, and cortico-striatal projections. This analysis did not reveal any difference between UCP and TD children at the level of other subcortical structures, such as basal ganglia or brainstem.

3.5. Results of q-BTS analysis

The q-BTS performed at ROI level revealed, except for frontal and parietal lobes ROIs, the presence of lower volume of gray and white matter in UCP patients as compared with TD control participants (Suppl. Table 6). In UCP patients, a significant relation was present between volume of subcortical structures and the level of unimanual and bimanual ability (Fig. 5 and Suppl. Table 7A). In particular, MUUL score correlates positively with the volume (FIRST segmentation, Fig. 5A-B) of the composite basal ganglia/brainstem/thalamus ROI (BG-BS-Thal) ($R^2 = 0.59$; $p = 0.008$), caudate nucleus ($R^2 = 0.55$; $p = 0.001$), putamen ($R^2 = 0.51$; $p = 0.002$) thalamus ($R^2 = 0.80$; $p < 0.001$) and brainstem nuclei ($R^2 = 0.29$; $p = 0.03$). Similarly, also the AHA score (Fig. 5C) positively correlates with volume of BG-BS-Thal ($R^2 = 0.40$; $p = 0.01$), caudate nucleus ($R^2 = 0.31$; $p = 0.04$), putamen ($R^2 = 0.35$; $p = 0.01$), and thalamus ($R^2 = 0.49$; $p = 0.003$).

Concerning the manipulation pattern, UCP patients with synergic hand showed lower gray matter volume of BG-BS-Thal (Mann-Whitney $U = 9$, $p = 0.02$), caudate nucleus (Mann-Whitney $U = 8$, $p = 0.02$), putamen (Mann-Whitney $U = 6$, $p = 0.009$), and thalamus (Mann-Whitney $U = 1$, $p < 0.001$) as compared to patients with semi-functional hand (Fig. 5D and Suppl. Table 8A). Concerning the gestational age, no differences in gray matter q-BTS scores were evident between UCP patients born at term and patients born preterm (Suppl. Table 8A).

The q-BTS analysis carried out on white matter ROIs (Fig. 6) revealed a positive correlation between MUUL score and volume of IL hemisphere white matter ($R^2 = 0.36$; $p = 0.01$), corticospinal tract ($R^2 = 0.27$; $p = 0.04$), white matter in the brainstem ($R^2 = 0.29$; $p = 0.03$), and fronto-striatal projections ($R^2 = 0.85$; $p < 0.001$) (Suppl. Table 7B). No significant relation with AHA score was found, considering the white matter analysis. Concerning the manipulation pattern, UCP patients with synergic hand showed lower volume of fronto-striatal projections, as compared to UCP children with semi-functional hand (Mann-Whitney $U = 3$, $p = 0.002$) (Suppl. Table 8B).

3.6. Functional activation during motor task

Head motion parameters acquired during the scanning session show that displacement in all planes was < 2 mm and comparable in the two groups of UCP patients with semi-functional and synergic hand (see Suppl. Fig. 6). All patients presented significant activation during both *Exe Grasp* and *Exe Move* motor tasks. In all cases except for patient 08 (normotensive hydrocephalus; Lesion Type II, outlier excluded from the analysis), cluster peaks were evident at the level of sensorimotor cortex in the IL hemisphere (see Fig. 7).

Concerning the activated areas, during *Exe Grasp*, UCP patients showed preserved activation of primary sensorimotor areas (M1/S1), secondary somatosensory area (SII), premotor cortex, supplementary motor area (SMA), and inferior parietal cortex (IPL) in the IL hemisphere (Fig. 8A). Activations were also evident in the contralesional hemisphere, at the level of the IPL, intraparietal sulcus (IPS), ventral and dorsal sector of premotor cortex (PMv, PMd) and dorsolateral prefrontal cortex (dlPFC). During *Exe Move*, patients showed less extended activations, more focused at the level of M1/S1 in the IL hemisphere. Other clusters in the CL hemisphere included PMd, PMv, and SMA. The direct contrast between *Exe Grasp* vs *Exe Move* revealed higher activations of IPL and IPS both in the IL and in CL hemisphere, and a cluster at the level of the IL SMA (Fig. 8A).

The lateralization index (LI) calculated in the whole sample of UCP patients, revealed activations lateralized in the IL hemisphere during both *Exe Grasp* (LI = 0.66; SD = 0.26) and *Exe Move* (LI = 0.85; SD = 0.20). No significant relation was found between lateralization of activation peak and the lesion type according with Cioni et al. classification ($R^2 = 0.16$; $p = 0.13$). Considering the whole sample, a significant difference was present between the two tasks, with activations more lateralized during *Exe Move* as compared with *Exe Grasp* (Mann-Whitney $U = 51.01$; $p = 0.009$) (Fig. 8B).

Non-parametric ANOVA showed a significant interaction between LI during the two tasks (*Exe Grasp, Exe Move*) and the type of kinematic hand pattern (*synergic, semi-functional*) (Kruskal-Wallis rank test = 10.08, $p = 0.01$) (Fig. 8C). Post hoc comparisons showed that UCP children with *semi-functional hand* had more bilateral activations during *Exe Grasp* (LI = 0.49, SD = 0.25) as compared with *Exe Move* (LI = 0.85, SD = 0.33) ($p = 0.01$). No significant difference was found in UCP children with *synergic hand*, showing a comparable lateralization during both tasks (*Exe Grasp* LI = 0.81, SD = 0.18; *Exe Move* LI = 0.86, SD = 0.20) ($p = 0.99$) (Fig. 8C). A very similar result was obtained by calculating LI using a whole-brain approach (see Suppl. Fig. 7).

Finally, in the whole sample, LI during *Exe Grasp* was linearly related to measures of unimanual (MUUL; $R^2 = 0.27$; $p = 0.04$) (Fig. 8D) and bimanual functions (AHA; $R^2 = 0.28$; $p = 0.04$) (Fig. 8E), confirming that patients with better motor abilities showed more bilateral activations.

4. Discussion

The main objective of the present study was to investigate lesion topography and preserved brain areas in UCP children with specific patterns of hand manipulation, i.e., *synergic* hand and *semi-functional* hand. Overall, our findings confirm previous works on brain structures most frequently damaged in UCP children, better describing the relation between damage of specific cortical and subcortical structures and functional impairment in hand manipulation. A common result emerging from the different qualitative and quantitative methodologies we used is the involvement of subcortical structures, predicting unimanual and bimanual residual motor ability. In addition, our fMRI results allow to characterize a differential reorganization of the activated motor networks during execution of grasping actions and simple movements, showing that children with *semi-functional* hand tend to recruit more bilateral areas during grasping execution, while children with *synergic* hand show activations more lateralized in the ipsilesional hemisphere, contralateral to the more affected hand.

4.1. Relation between brain lesion and manipulation pattern

Concerning presumed timing, the lesions found in the present cohort of patients can be classified in most cases as Type II/III (prenatal-connatal) (Cioni et al., 1999). Only one patient showed a Type I lesion (early malformative). This prevalence of lesion types is in line with previous similar works (Cioni et al., 1999; Sgandurra et al., 2018). However, no direct relation was found between specific patterns of manipulation and lesion timing or gestational age (born preterm vs. at term). This finding confirms that, beyond the presumed timing, lesion localization (in terms of involved structures and white matter connections) is very likely a relevant factor to explain the difference in manipulation ability.

Lesion overlap analysis confirmed the involvement of several regions, including periventricular white matter, posterior sector of corpus callosum, posterior limb of the internal capsule, thalamus, basal ganglia, and brainstem. The sq-MRI classification confirmed that in most patients

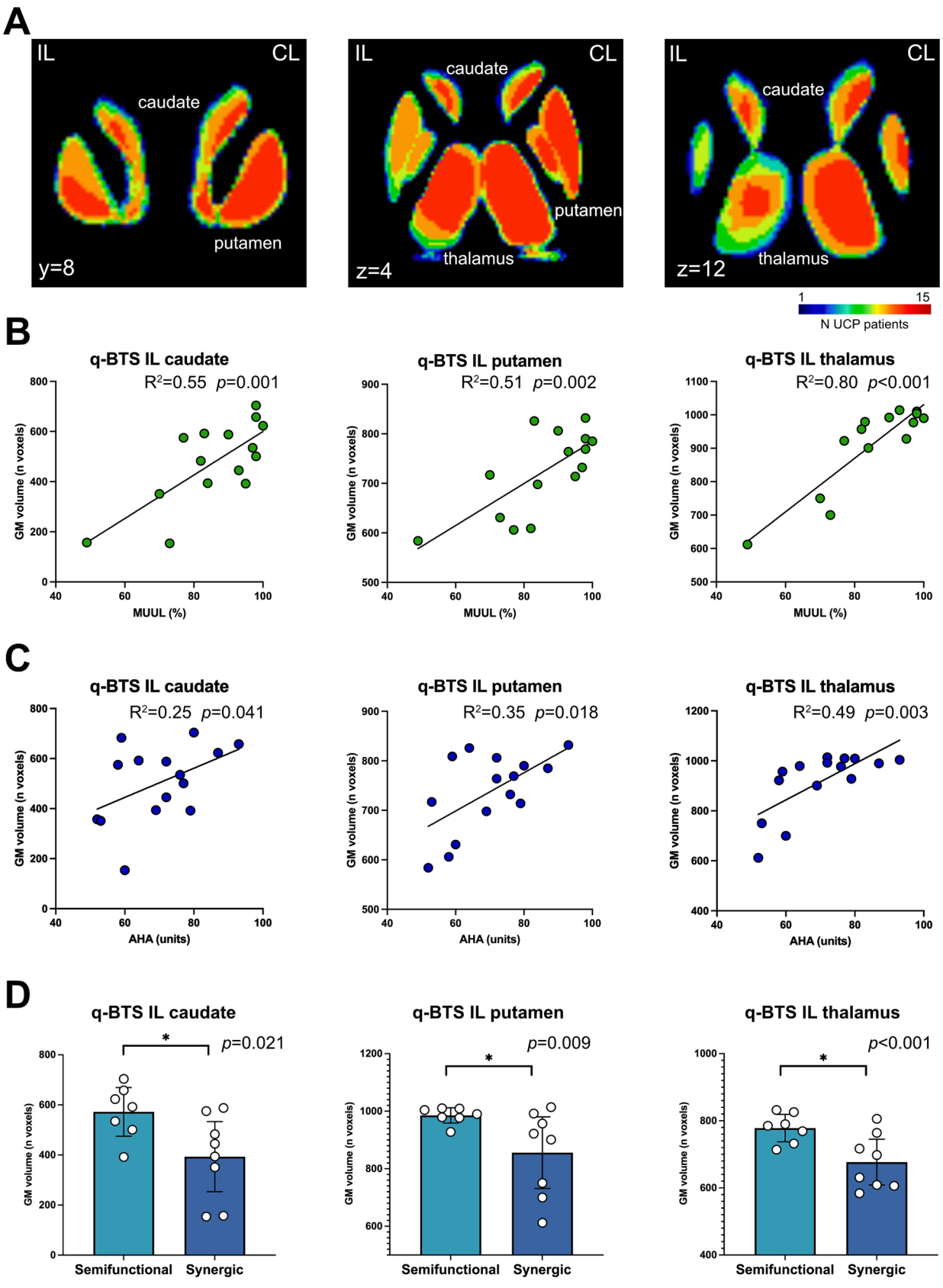

Fig. 5. Results of regression analysis performed on q-BTS based on subcortical nuclei segmentation. (A) Average map of gray matter distribution related to subcortical structures (FIRST-FSL segmentation) in UCP patients. The map is visualized on two axial and one coronal representative sections of subcortical nuclei. (B) Scatterplots show significant linear relation between volume of subcortical structures and unimanual ability (MUUL score). (C) Linear regressions between volume of subcortical structures and bimanual function (AHA score). (D) Difference in subcortical nuclei volume in patients with *synergic* and *semi-functional* hand. Abbreviations: IL = ipsilesional hemisphere; CL = contralesional hemisphere.

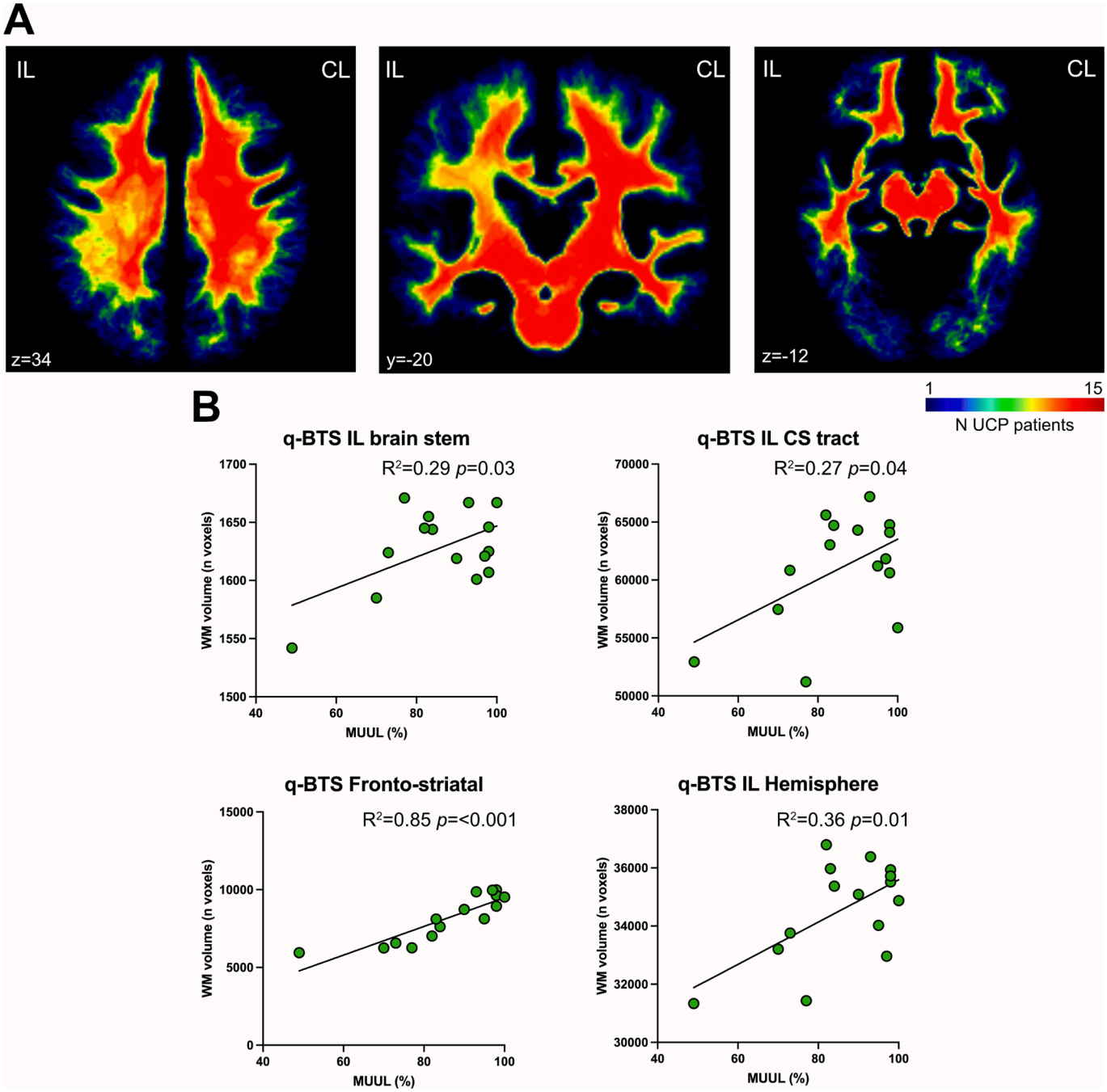

Fig. 6. Results of regression analysis performed on q-BTS based on white matter ROIs. (A) Average map of white matter distribution in UCP patients. (B) Scatterplots showing significant linear relation between volume of four white matter ROIs and unimanual ability (MUUL score). Abbreviations: IL = ipsilesional hemisphere; CL = contralesional hemisphere; CS = corticospinal tract; WM = white matter.

the lesions involved the ipsilesional white matter and subcortical structures. The same method revealed that lesions in patients with *synergic* hand involve more frequently the subcortical structures, as compared to patients with *semi-functional* hand. Furthermore, a correlation was evident between extent of lesions in subcortical structures and the scores obtained with measures of unimanual and bimanual ability, MUUL and AHA, respectively. This result is consistent with previous studies investigating all forms of CP, showing the relevance of the integrity of thalamus-basal ganglia-cortical circuits for developing a good motor function (Feys et al., 2010; Holmefur et al., 2013; Holmström et al., 2010). Considering that our cohort focused on UCP patients with mild or moderate hand impairment, findings demonstrate that the involvement of subcortical structures is relevant in these types of patients, too.

At the quantitative level, the comparison between segmented gray and white matter in UCP and TD children (VMB-DARTEL analysis) revealed subcortical lesions of white matter, similarly to what previously reported in other studies employing the same technique in UCP children (Scheck et al., 2014; Wang et al., 2015). However, it failed to identify lesions in subcortical nuclei such as basal ganglia or brainstem nuclei. A possible explanation for this negative finding is that whole-brain analysis is not sensitive enough to reveal the involvement of small subcortical structures. By integrating multiple imaging methods, it is possible to investigate specific involved structures. In fact, we employed a tissue segmentation (q-BTS) ROI-based analysis performed on the segmented cortical gray matter and subcortical nuclei, showing a

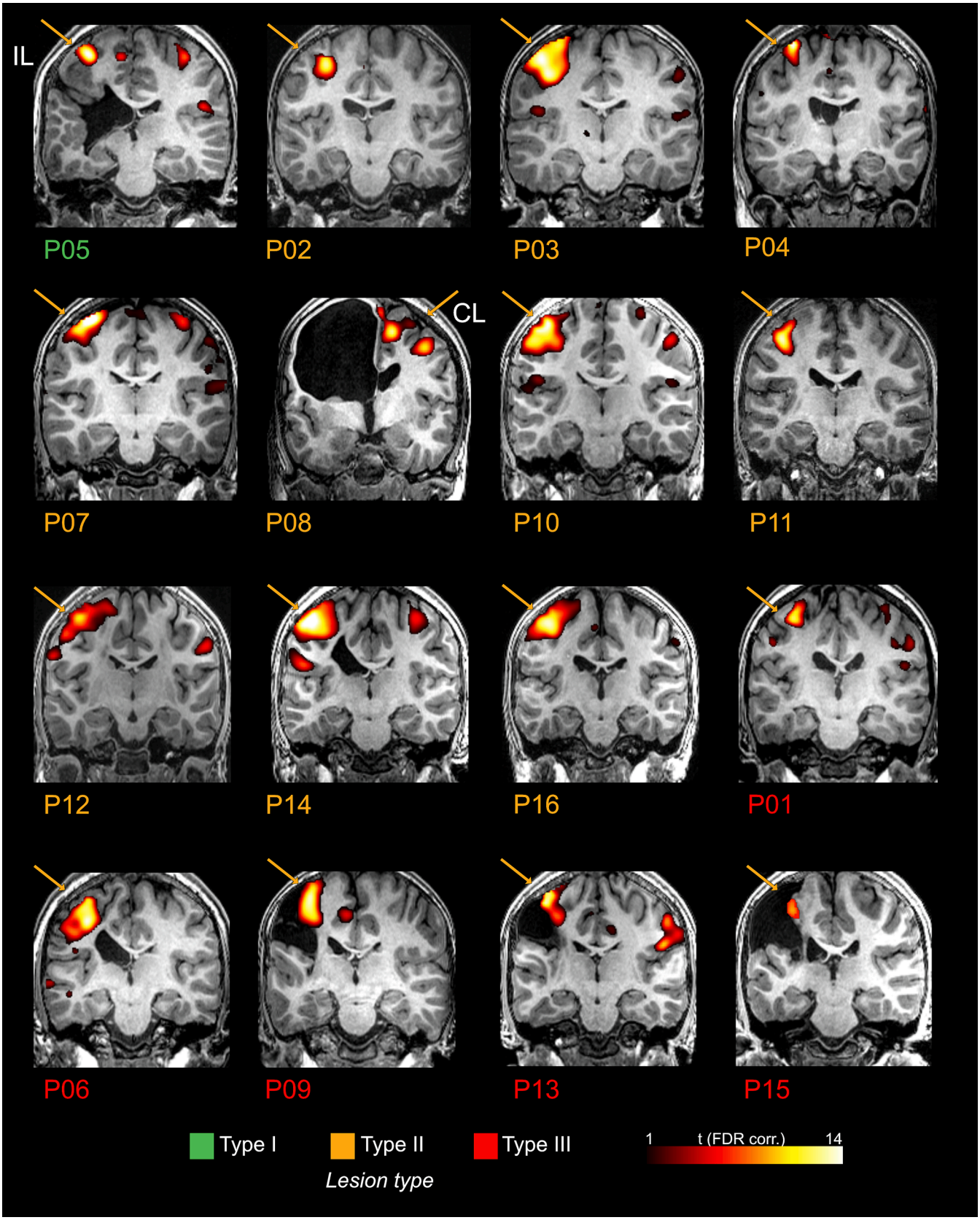

Fig. 7. Single-subject activations during execution of grasping acts (Exe Grasp) overlaid on individual coronal sections of T1-w images. Orange arrows indicate the prevalent activated side, considering cluster peak at the level of the primary sensorimotor cortex. Patients are also grouped according with lesion type classification by Cioni et al. (1999). IL = ipsilesional hemisphere.

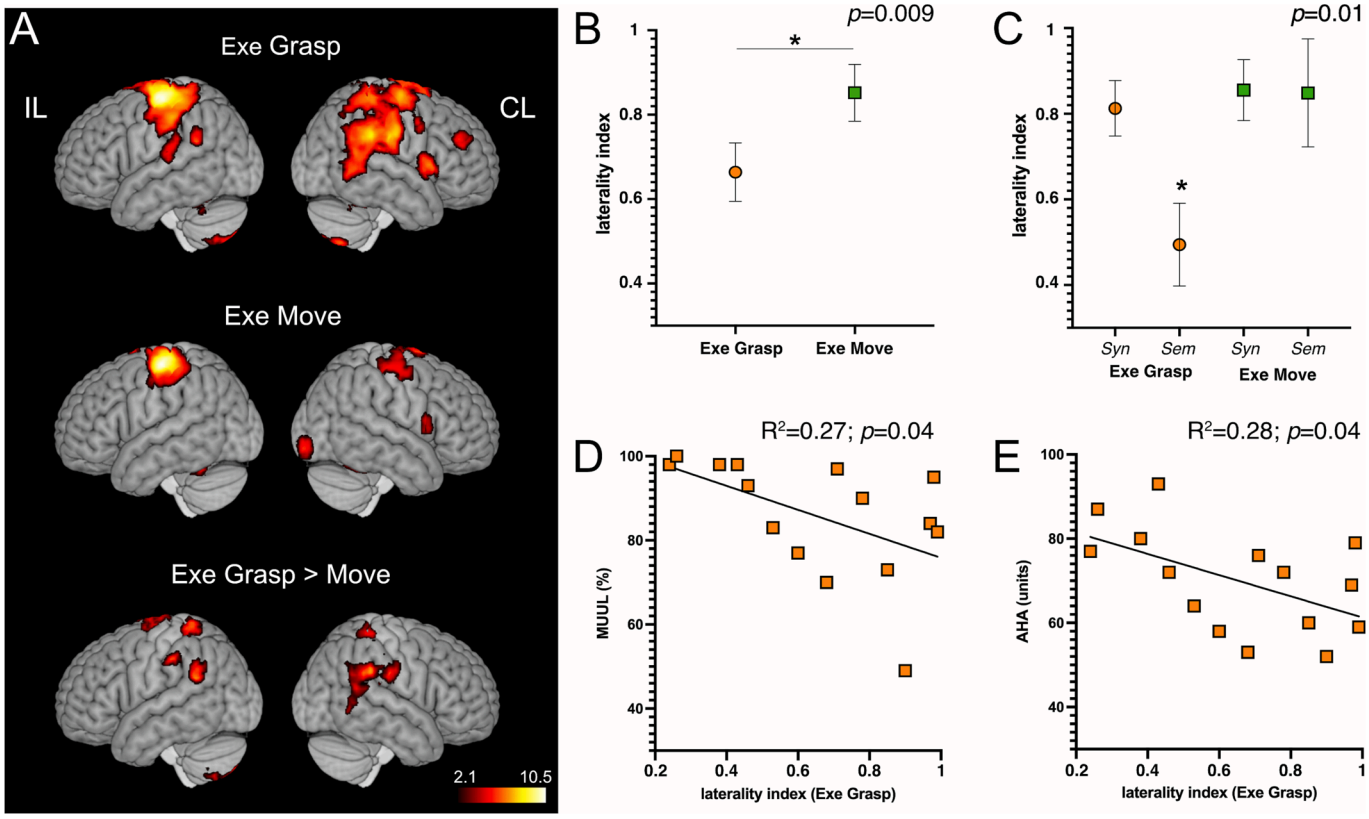

Fig. 8. Brain activation in UCP children during motor task. (A) Statistical parametric maps of activation are overlaid into a standard MNI pediatric template. IL = ipsilesional hemisphere; CL = contralesional hemisphere. (B) Laterality index (LI) related to the activation of sensorimotor cortex during *Exe Grasp* and *Exe Move* conditions in the whole sample. A significant difference was present between the two tasks, with activations more lateralized during *Exe Move* as compared with *Exe Grasp*. (C) LI calculated in UCP children with *synergic hand* (syn) and *semi-functional hand* (sem) kinematic pattern. Non-parametric ANOVA showed that UCP children with *semi-functional* hand had more bilateral activations during *Exe Grasp* as compared with *Exe Move*. On the contrary, no significant difference was found in UCP children with *synergic* hand, showing a comparable lateralization during both tasks. (D-E) Significant linear relation between LI during *Exe Grasp* and MUUL score and AHA score, respectively. This indicates that patients with better motor abilities showed more bilateral activations.

positive linear relationship between the volume of subcortical nuclei (particularly the caudate, putamen, and thalamus) and MUUL and AHA scores. In addition, patients with *synergic* hand showed lower volume of the same subcortical nuclei as compared to patients with *semi-functional* hand. This latter result indicates that the integrity of subcortical structures not only contribute to development of motor ability during unimanual hand-object interaction, but also to integrate the use of more affected and less affected hands to produce a correct motor output. On the contrary, no specific relation was found using cortical areas as ROIs.

The q-BTS analysis on the segmented white matter revealed that volume of fronto-striatal projections was lower in patients with *synergic* hand as compared to those with *semi-functional* hand. Moreover, a positive relation was present between the volume of spared white matter in the ipsilesional hemisphere and the score obtained on the MUUL scale. In particular, this relationship emerged when comparing MUUL score and volume of ipsilesional corticospinal tract, fronto-striatal tract and the white matter of brainstem. However, no relationship was found between volume of spared white matter and AHA score. This result represents first indirect evidence of the underlying motor reorganization in our cohort of patients, suggesting very likely a contralateral reorganization (see Fig. 9), in which the more affected hand is still controlled by the contralateral, lesioned hemisphere. Accordingly, it emerged that preservation of white matter connections originating from the lesioned hemisphere predicts mainly the unimanual ability, as assessed with MUUL scale. The lower volume of fronto-striatal connections in patients with *synergic* hand confirms the results obtained with sq-MRI lesion classification concerning the involvement of basal ganglia. Overall, our findings are in line with previous investigation showing that structural connectivity of these pathways is reduced in children with poorer bimanual performance and unimanual capacity (Fiori et al., 2015; Mackey et al., 2014; Pannek et al., 2014; Reid et al., 2016). The interesting finding is that a range of spared structural connections can also be present in children with mild to moderate impairment, and that it is possible to reveal a difference between them, in significant relation with their respective manipulation pattern. It could be interesting to deeply investigate, in patients showing contralateral reorganization, the contribution of possible spared crossed fronto-striatal fibers connecting the contralesional motor cortex with the ipsilesional striatum, as described by recent neuroanatomical studies in monkey (Borra et al., 2022). Noteworthy, it has been demonstrated, in rodents with a unilateral lesion of motor cortex, the presence of crossed projections between contralesional motor cortex and ipsilesional striatum (Napieralski et al., 1996; Uryu et al., 2001).

4.2. *Relation between functional activation during grasping execution and manipulation pattern*

Concerning the fMRI study, a first finding is the demonstration that motor reorganization in UCP patients can be investigated not only with passive movements or simple hand opening/closing tasks (Gaberova et al., 2018), but also with more complex tasks, such as grasping actions. Our simple movements task provides a picture comparable to that reported in the literature for patients with small lesions (Staudt, 2007; Staudt et al., 2002) (Fig. 9), with clear activation of the ipsilesional primary motor cortex (MI) and of contralesional premotor and parietal areas. Only one patient showed a complete ipsilateral reorganization

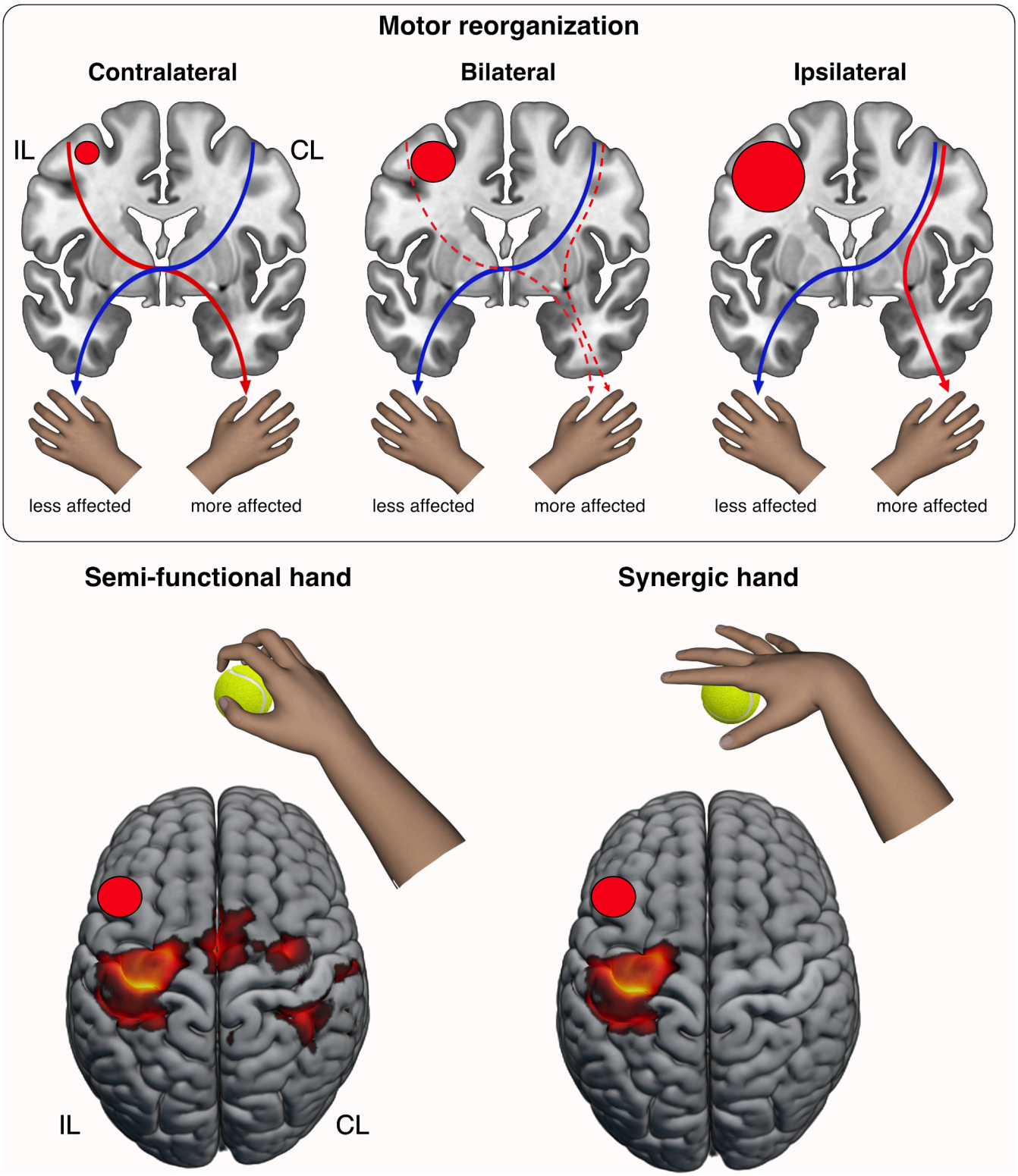

Fig. 9. Upper panel, schematic representation of the most common types of motor reorganization observed in UCP children. Red circles indicate the location of the main lesion, and the circle diameter represents lesions with different size. In the contralateral reorganization, motor function reorganizes in the ipsilesional hemisphere. Red arrows represent structural connections controlling the more affected hand, while blue arrows represent connections to the less affected hand. In bilateral type of reorganization, a significant number of monosynaptic fast conducting projections from the undamaged cortex persists. Dotted arrows represent the spared connections between the ipsilesional hemisphere and the more affected hand, plus fast conducting projections from the undamaged cortex, typically described in this form of motor reorganization. In cases of complete ipsilateral reorganization, the more affected hand is mainly controlled by the ipsilateral undamaged cortex. Lower panel, functional activations observed in patients with *semi-functional* and *synergic* manipulation pattern during grasping execution. IL = ipsilesional hemisphere, CL = contralesional hemisphere.

(hydrocephalus and Type II lesion). In all other cases, including those showing cortical lesions, a contralateral reorganization was observed, with spared activation in the ipsilesional hemisphere, regardless of the lesion type (Cioni et al., 1999).

Previous evidence showed that children with ipsilateral reorganization (in which the more affected hand is controlled by the ipsilateral hemisphere through fast-conducting ipsilateral corticospinal projections) (Fig. 9) have a more impaired upper limb compared to children with contralateral reorganization (in which the more affected hand is still controlled by the spared contralateral motor cortex through corticospinal projections) (Holmström et al., 2010; Mackey et al., 2014; Simon-Martinez et al., 2018). Furthermore, other studies suggested that the reorganization of the corticospinal tract is the strongest determinant of upper limb motor function in UCP, contributing significantly to the existing variability in hand function (Mailleux et al., 2020; Simon-Martinez et al., 2018). Our results are in line with this evidence, since all patients, but one, showed a contralateral reorganization, associated with mild or moderate hand impairment, that presents two patterns of hand manipulation differing in strategy and kinematic features.

Considering the whole sample of patients, during the grasping task, functional activations were more bilateral as compared to activation during simple movement task. The contrast between grasping and simple movement tasks showed greater activation in dorsal premotor cortex, superior and inferior parietal lobules. These activations are possibly related to the processing of action goals and, perhaps, also of movement kinematics, as previously demonstrated in studies on healthy children and adults (Biagi et al., 2016; Errante et al., 2021; Gazzola et al., 2007).

When comparing children with *synergic* and *semi-functional* hand, it emerges that the former show more lateralized activation in the ipsilesional hemisphere both during execution of grasping and simple movements, while the latter had a different pattern of activation when performing grasping execution or simple movements, namely more bilateral activation during grasping and more lateralized activation during simple movements (Fig. 9). These data integrate previous studies, suggesting that more impaired patients would exhibit a shift of activation to the hemisphere ipsilateral to the more affected hand (Staudt, 2007; Weinstein et al., 2014). The evidence that patients with a more restricted repertoire, namely *synergic* pattern, show greater lateralization to the lesioned hemisphere could be explained by a tendency to simplify motor schemes, according to the logic of synergy that characterizes this hand pattern. Therefore, the *synergic* hand has fewer strategies, while the *semi-functional* hand has more potential for modification and the ability to combine modules (Ferrari & Cioni, 2010) (see also Suppl. Table 1 for a description of the main kinematic features of this manipulation pattern). The bilateral activation included areas of the contralesional hemisphere known to be involved in planning and execution of grasping actions, such as IPL, IPS, PMd, PMv, plus dorsolateral prefrontal cortex (dlPFC). These areas should be reciprocally interconnected with the ipsilesional cortex through callosal connections (Marconi et al., 2003; Park et al., 2008). Thus, in children with *semi-functional* hand, it is possible that during execution of grasping actions, this bilateral activation improves some kinematic features of the manipulation pattern and allows combination of modules.

4.3. Limitation and future directions

In the present study, it was not possible to acquire data regarding a control group of children matched by age. These data would be fundamental to better interpret the fMRI results obtained in UCP patients. Regarding the fMRI assessment, in future studies it would be interesting to evaluate the change in functional lateralization during the use of the less affected hand, and verify whether the motor skills of the two hands are differently influenced by the type of lesion and by specific manipulation pattern. Another possible limitation of the present study is that we did not use TMS to record the type of corticospinal tract wiring, which, in combination with underlying lesion location/extent, has been shown to influence upper limb motor function. Furthermore, when combined with TMS, the use of advanced techniques based on Diffusion Tensor Imaging (DTI) allows to detect, localize, and quantify subtle brain white matter abnormalities that may not be visible on conventional structural MRI (Mailleux et al., 2020; Pannek et al., 2014; Reid et al., 2016). This could reveal a relationship between the microstructural properties of motor tracts and specific hand manipulation patterns. By using task-fMRI, we were able to obtain a more comprehensive functional characterization, which indeed reveals the activation of parieto-premotor circuits that reflect how the goal and kinematics of actions are processed in UCP patients. Future studies employing a multimodal approach should consider both the imaging of the activation pattern (fMRI) and the potential contribution of corticospinal tract wiring (TMS/DTI) (Weinstein et al., 2018).

From a translational clinical perspective, our findings could represent important advances for understanding the brain mechanisms responsible for motor improvement observed in UCP children after the application of treatments based on action observation and imitation, i.e., the so-called Action Observation Treatment (AOT) (Buccino, 2014; Sgandurra et al., 2013, 2020; Verzelloni et al., 2021). In fact, there are no studies differentiating the effects of AOT in terms of motor improvement in children with *synergic* and *semi-functional* hand. Future investigations should consider the manipulation pattern, to personalize the treatment based on individual kinematic features of the more affected hand. Based on our finding, improvements in both unimanual and bimanual functions after AOT, in patients with *synergic* hand, may be associated with the acquisition of greater bilateral functional activation of the sensorimotor circuits. In addition, it remains to be clarified if patients with preserved activation of basal ganglia could present, after AOT, increased functional connectivity between contralesional motor cortex and ipsilesional striatum.

Funding

This study was funded by a grant from Chiesi Farmaceutici S.p.A. (Parma, IT). However, nobody from Chiesi Farmaceutici had a role in the design of the study or in writing this manuscript.

CRediT authorship contribution statement

Antonino Errante: Conceptualization, Data curation, Formal analysis, Investigation, Methodology, Visualization, Writing – original draft, Writing – review & editing. **Francesca Bozzetti:** Conceptualization, Data curation, Investigation, Writing – review & editing. **Alessandro Piras:** Formal analysis, Visualization, Writing – review & editing. **Laura Beccani:** Investigation, Writing – review & editing. **Mariacristina Filippi:** Investigation, Writing – review & editing. **Stefania Costi:** Investigation, Writing – review & editing. **Adriano Ferrari:** Resources, Supervision, Writing – review & editing. **Leonardo Fogassi:** Conceptualization, Funding acquisition, Project administration, Supervision, Writing – review & editing.

Declaration of competing interest

The authors declare that they have no known competing financial interests or personal relationships that could have appeared to influence the work reported in this paper.

Data availability

Data will be made available on request.

Acknowledgements

We gratefully acknowledge the participating children and their parents.

Ethics approval statement

The study was approved by the local ethics committee (Comitato Etico Area Vasta Emilia Nord – AVEN). This study was carried out in accordance with The Code of Ethics of the World Medical Association (Declaration of Helsinki). Parental written informed consent for all participants was obtained.

Appendix A. Supplementary data

Supplementary data to this article can be found online at https://doi.org/10.1016/j.nicl.2024.103575.

References

Ashburner, J., 2007. A fast diffeomorphic image registration algorithm. Neuroimage 38 (1), 95–113. https://doi.org/10.1016/j.neuroimage.2007.07.007.

Ashburner, J., Friston, K.J., 2005. Unified segmentation. Neuroimage 26 (3), 839–851. https://doi.org/10.1016/j.neuroimage.2005.02.018.

Bax, M., Goldstein, M., Rosenbaun, P., Leviton, A., Paneth, N., Dan, B., Jacobsson, B., Damiano, D., 2005. Proposed definition and classification of cerebral palsy, April 2005. Dev. Med. Child Neurol. 47 (8), 571. https://doi.org/10.1017/S001216220500112X.

Biagi, L., Cioni, G., Fogassi, L., Guzzetta, A., Sgandurra, G., Tosetti, M., 2016. Action observation network in childhood: a comparative fMRI study with adults. Dev. Sci. 19 (6), 1075–1086. https://doi.org/10.1111/DESC.12353.

Borra, E., Biancheri, D., Rizzo, M., Leonardi, F., Luppino, G., 2022. Crossed Corticostriatal Projections in the Macaque Brain. J. Neurosci. 42 (37), 7060–7076. https://doi.org/10.1523/JNEUROSCI.0071-22.2022.

Buccino, G., 2014. Action observation treatment: A novel tool in neurorehabilitation. Philos. Trans. R. Soc., B 369 (1644), 20130185. https://doi.org/10.1098/rstb.2013.0185.

Cioni, G., Sales, B., Paolicelli, P.B., Petacchi, E., Scusa, M.F., Canapicchi, R., 1999. MRI and clinical characteristics of children with hemiplegic cerebral palsy. Neuropediatrics 30 (5), 249–255. https://doi.org/10.1055/S-2007-973499.

Crichton, A., Ditchfield, M., Gwini, S., Wallen, M., Thorley, M., Bracken, J., Harvey, A., Elliott, C., Novak, I., Hoare, B., 2020. Brain magnetic resonance imaging is a predictor of bimanual performance and executive function in children with unilateral cerebral palsy. Dev. Med. Child Neurol. 62 (5), 615–624. https://doi.org/10.1111/DMCN.14462.

Errante, A., Di Cesare, G., Pinardi, C., Fasano, F., Sghedoni, S., Costi, S., Ferrari, A., Fogassi, L., 2019. Mirror neuron system activation in children with unilateral cerebral palsy during observation of actions performed by a pathological model. Neurorehabil. Neural Repair 33 (6), 419–431. https://doi.org/10.1177/1545968319847964.

Errante, A., Ziccarelli, S., Mingolla, G.P., Fogassi, L., 2021. Decoding grip type and action goal during the observation of reaching-grasping actions: A multivariate fMRI study. Neuroimage 243. https://doi.org/10.1016/J.NEUROIMAGE.2021.118511.

Ferrari, A., Cioni, G., 2010. The Spastic forms of cerebral palsy: A guide to the assessment of adaptive functions. The Spastic Forms of Cerebral Palsy: A Guide to the Assessment of Adaptive Functions 1–359. https://doi.org/10.1007/978-88-470-1478-7/COVER.

Feys, H., Eyssen, M., Jaspers, E., Klingels, K., Desloovere, K., Molenaers, G., De Cock, P., 2010. Relation between neuroradiological findings and upper limb function in hemiplegic cerebral palsy. Eur. J. Paediatr. Neurol. 14 (2), 169–177. https://doi.org/10.1016/J.EJPN.2009.01.004.

Fiori, S., Cioni, G., Klingels, K., Ortibus, E., Van Gestel, L., Rose, S., Boyd, R.N., Feys, H., Guzzetta, A., 2014. Reliability of a novel, semi-quantitative scale for classification of structural brain magnetic resonance imaging in children with cerebral palsy. Dev. Med. Child Neurol. 56 (9), 839–845. https://doi.org/10.1111/DMCN.12457.

Fiori, S., Guzzetta, A., Pannek, K., Ware, R.S., Rossi, G., Klingels, K., Feys, H., Coulthard, A., Cioni, G., Rose, S., Boyd, R.N., 2015. Validity of semi-quantitative scale for brain MRI in unilateral cerebral palsy due to periventricular white matter lesions: Relationship with hand sensorimotor function and structural connectivity. NeuroImage. Clinical 8, 104–109. https://doi.org/10.1016/J.NICL.2015.04.005.

Fonov, V., Evans, A.C., Botteron, K., Almli, C.R., McKinstry, R.C., Collins, D.L., 2011. Unbiased average age-appropriate atlases for pediatric studies. Neuroimage 54 (1), 313. https://doi.org/10.1016/J.NEUROIMAGE.2010.07.033.

Foulon, C., Cerliani, L., Kinkingnéhun, S., Levy, R., Rosso, C., Urbanski, M., Volle, E., de Schotten, M.T., 2018. Advanced lesion symptom mapping analyses and implementation as BCBtoolkit. GigaScience 7 (3), 1–17. https://doi.org/10.1093/gigascience/giy004.

Franki, I., Mailleux, L., Emsell, L., Peedima, M.L., Fehrenbach, A., Feys, H., Ortibus, E., 2020. The relationship between neuroimaging and motor outcome in children with cerebral palsy: A systematic review - Part A Structural Imaging. *Res. Dev. Disabil.* 100 https://doi.org/10.1016/J.RIDD.2020.103606.

Friston, K.J., Holmes, A.P., Worsley, K.J., Poline, J.-P., Frith, C.D., Frackowiak, R.S.J., 1994. Statistical parametric maps in functional imaging: A general linear approach. Hum. Brain Mapp. 2 (4), 189–210. https://doi.org/10.1002/HBM.460020402.

Gaberova, K., Pacheva, I., Ivanov, I., 2018. Task-related fMRI in hemiplegic cerebral palsy-A systematic review. J. Eval. Clin. Pract. 24 (4), 839–850. https://doi.org/10.1111/JEP.12929.

Gazzola, V., Rizzolatti, G., Wicker, B., Keysers, C., 2007. The anthropomorphic brain: The mirror neuron system responds to human and robotic actions. Neuroimage 35 (4), 1674–1684. https://doi.org/10.1016/j.neuroimage.2007.02.003.

Guzzetta, A., Bonanni, P., Biagi, L., Tosetti, M., Montanaro, D., Guerrini, R., Cioni, G., 2007. Reorganisation of the somatosensory system after early brain damage. Clin. Neurophysiol. 118 (5), 1110–1121. https://doi.org/10.1016/j.clinph.2007.02.014.

Holmefur, M., Krumlinde-Sundholm, L., Eliasson, A.C., 2007. Interrater and intrarater reliability of the assisting hand assessment. Am. J. Occup. Ther. 61 (1), 79–84. https://doi.org/10.5014/AJOT.61.1.79.

Holmefur, M., Kits, A., Bergström, J., Krumlinde-Sundholm, L., Flodmark, O., Forssberg, H., Eliasson, A.C., 2013. Neuroradiology can predict the development of hand function in children with unilateral cerebral palsy. Neurorehabil. Neural Repair 27 (1), 72–78. https://doi.org/10.1177/1545968312446950.

Holmström, L., Vollmer, B., Tedroff, K., Islam, M., Persson, J.K.E., Kits, A., Forssberg, H., Eliasson, A.C., 2010. Hand function in relation to brain lesions and corticomotor-projection pattern in children with unilateral cerebral palsy. Dev. Med. Child Neurol. 52 (2), 145–152. https://doi.org/10.1111/J.1469-8749.2009.03496.X.

House, J.H., Gwathmey, F.W., Fidler, M.O., 1981. A dynamic approach to the thumb-in palm deformity in cerebral palsy. J. Bone Joint Surg. Am. 63 (2), 216–225. https://doi.org/10.2106/00004623-198163020-00006.

Klingels, K., Demeyere, I., Jaspers, E., De Cock, P., Molenaers, G., Boyd, R., Feys, H., 2012. Upper limb impairments and their impact on activity measures in children with unilateral cerebral palsy. Eur. J. Paediatr. Neurol. 16 (5), 475–484. https://doi.org/10.1016/J.EJPN.2011.12.008.

Koman, L.A., Williams, R.M.M., Evans, P.J., Richardson, R., Naughton, M.J., Passmore, L., Smith, B.P., 2008. Quantification of upper extremity function and range of motion in children with cerebral palsy. Dev. Med. Child Neurol. 50 (12), 910–917. https://doi.org/10.1111/J.1469-8749.2008.03098.X.

Korzeniewski, S.J., Birbeck, G., DeLano, M.C., Potchen, M.J., Paneth, N., 2008. A systematic review of neuroimaging for cerebral palsy. J. Child Neurol. 23 (2), 216–227. https://doi.org/10.1177/0883073807307983.

Krägeloh-Mann, I., 2004. Imaging of early brain injury and cortical plasticity. Exp. Neurol. 190 (SUPPL. 1), 84–90. https://doi.org/10.1016/j.expneurol.2004.05.037.

Krägeloh-Mann, I., Horber, V., 2007. The role of magnetic resonance imaging in elucidating the pathogenesis of cerebral palsy: A systematic review. In Developmental Medicine and Child Neurology (Vol. 49, Issue 2, pp. 144–151). John Wiley & Sons, Ltd. https://doi.org/10.1111/j.1469-8749.2007.00144.x.

Krägeloh-Mann, I., Cans, C., 2009. Cerebral palsy update. Brain Dev. 31 (7), 537–544. https://doi.org/10.1016/J.BRAINDEV.2009.03.009.

Louwers, A., Krumlinde-Sundholm, L., Boeschoten, K., Beelen, A., 2017. Reliability of the Assisting Hand Assessment in adolescents. Dev. Med. Child Neurol. 59 (9), 926–932. https://doi.org/10.1111/DMCN.13465.

Mackey, A., Stinear, C., Stott, S., Byblow, W.D., 2014. Upper limb function and cortical organization in youth with unilateral cerebral palsy. Front. Neurol. 5 https://doi.org/10.3389/FNEUR.2014.00117.

Mailleux, L., Klingels, K., Fiori, S., Simon-Martinez, C., Demaerel, P., Locus, M., Fosseprez, E., Boyd, R.N., Guzzetta, A., Ortibus, E., Feys, H., 2017. How does the interaction of presumed timing, location and extent of the underlying brain lesion relate to upper limb function in children with unilateral cerebral palsy? Eur. J. Paediatr. Neurol. 21 (5), 763–772. https://doi.org/10.1016/J.EJPN.2017.05.006.

Mailleux, L., Simon-Martinez, C., Radwan, A., Blommaert, J., Gooijers, J., Wenderoth, N., Klingels, K., Ortibus, E., Sunaert, S., Feys, H., 2020. White matter characteristics of motor, sensory and interhemispheric tracts underlying impaired upper limb function in children with unilateral cerebral palsy. Brain Struct. Funct. 225 (5), 1495–1509. https://doi.org/10.1007/S00429-020-02070-1.

Maldjian, J.A., Laurienti, P.J., Kraft, R.A., Burdette, J.H., 2003. An automated method for neuroanatomic and cytoarchitectonic atlas-based interrogation of fMRI data sets. Neuroimage 19 (3), 1233–1239. https://doi.org/10.1016/S1053-8119(03)00169-1.

Marconi, B., Genovesio, A., Giannetti, S., Molinari, M., Caminiti, R., 2003. Callosal connections of dorso-lateral premotor cortex. Eur. J. Neurosci. 18 (4), 775–788. https://doi.org/10.1046/J.1460-9568.2003.02807.X.

Motulsky, H.J., Brown, R.E., 2006. Detecting outliers when fitting data with nonlinear regression – a new method based on robust nonlinear regression and the false discovery rate. BMC Bioinf. 7, 123. https://doi.org/10.1186/1471-2105-7-123.

Napieralski, J.A., Butler, A.K., Chesselet, M.-F., 1996. Anatomical and functional evidence for lesion-specific sprouting of corticostriatal input in the adult rat. J. Comp. Neurol. 373, 484–497. https://doi.org/10.1002/(SICI)1096-9861(19960930)373:4.

Oskoui, M., Coutinho, F., Dykeman, J., Jetté, N., Pringsheim, T., 2013. An update on the prevalence of cerebral palsy: a systematic review and meta-analysis. Dev. Med. Child Neurol. 55 (6), 509–519. https://doi.org/10.1111/DMCN.12080.

Pagnozzi, A.M., Pannek, K., Fripp, J., Fiori, S., Boyd, R.N., Rose, S., 2020. Understanding the impact of bilateral brain injury in children with unilateral cerebral palsy. Hum. Brain Mapp. 41 (10), 2794–2807. https://doi.org/10.1002/HBM.24978.

Pannek, K., Boyd, R.N., Fiori, S., Guzzetta, A., Rose, S.E., 2014. Assessment of the structural brain network reveals altered connectivity in children with unilateral cerebral palsy due to periventricular white matter lesions. NeuroImage. Clinical 5, 84–92. https://doi.org/10.1016/J.NICL.2014.05.018.

Park, H.J., Jae, J.K., Lee, S.K., Jeong, H.S., Chun, J., Dong, I.K., Jong, D.L., 2008. Corpus callosal connection mapping using cortical gray matter parcellation and DT-MRI. Hum. Brain Mapp. 29 (5), 503–516. https://doi.org/10.1002/HBM.20314.

Patenaude, B., Smith, S.M., Kennedy, D.N., Jenkinson, M., 2011. A Bayesian model of shape and appearance for subcortical brain segmentation. Neuroimage 56 (3), 907–922. https://doi.org/10.1016/j.neuroimage.2011.02.046.

Pueyo, R., Junqué, C., Vendrell, P., Narberhaus, A., Segarra, D., 2008. Raven's coloured progressive matrices as a measure of cognitive functioning in cerebral palsy. J. Intell.

Disab. Res.: JIDR 52 (Pt 5), 437–445. https://doi.org/10.1111/J.1365-2788.2008.01045.X.
Randall, M., Imms, C., Carey, L.M., Pallant, J.F., 2014. Rasch analysis of the melbourne assessment of unilateral upper limb function. Dev. Med. Child Neurol. 56 (7), 665–672. https://doi.org/10.1111/DMCN.12391.
Reid, L.B., Cunnington, R., Boyd, R.N., Rose, S.E., 2016. Surface-based fMRI-driven diffusion tractography in the presence of significant brain pathology: a study linking structure and function in cerebral palsy. PLoS One 11 (8). https://doi.org/10.1371/JOURNAL.PONE.0159540.
Robinson, M.N., Peake, L.J., Ditchfield, M.R., Reid, S.M., Lanigan, A., Reddihough, D.S., 2009. Magnetic resonance imaging findings in a population-based cohort of children with cerebral palsy. Dev. Med. Child Neurol. 51 (1), 39–45. https://doi.org/10.1111/J.1469-8749.2008.03127.X.
Rosenbaum, P., Paneth, N., Leviton, A., Goldstein, M., Bax, M., 2007. A report: The definition and classification of cerebral palsy April 2006. In Developmental Medicine and Child Neurology (Vol. 49, Issue SUPPL. 2, pp. 8–14). Blackwell Publishing Ltd. https://doi.org/10.1111/j.1469-8749.2007.tb12610.x.
Sakzewski, L., Ziviani, J., Boyd, R., 2010. The relationship between unimanual capacity and bimanual performance in children with congenital hemiplegia. Dev. Med. Child Neurol. 52 (9), 811–816. https://doi.org/10.1111/J.1469-8749.2009.03588.X.
Sanger, T.D., Delgado, M.R., Gaebler-Spira, D., Hallett, M., Mink, J.W., 2003. Classification and definition of disorders causing hypertonia in childhood. Pediatrics 111 (1), e89–e97. https://doi.org/10.1542/PEDS.111.1.E89.
Scheck, S.M., Pannek, K., Fiori, S., Boyd, R.N., Rose, S.E., 2014. Quantitative comparison of cortical and deep grey matter in pathological subtypes of unilateral cerebral palsy. Dev. Med. Child Neurol. 56 (10), 968–975. https://doi.org/10.1111/DMCN.12461.
Sellier, E., Platt, M.J., Andersen, G.L., Krägeloh-Mann, I., De La Cruz, J., Cans, C., Cans, C., Van Bakel, M., Arnaud, C., Delobel, M., Chalmers, J., McManus, V., Lyons, A., Parkes, J., Dolk, H., Himmelmann, K., Pahlman, M., Dowding, V., Colver, A., Mejaski-Bosnjak, V., 2016. Decreasing prevalence in cerebral palsy: a multi-site European population-based study, 1980 to 2003. Dev. Med. Child Neurol. 58 (1), 85–92. https://doi.org/10.1111/DMCN.12865.
Sgandurra, G., Ferrari, A., Cossu, G., Guzzetta, A., Fogassi, L., Cioni, G., 2013. Randomized trial of observation and execution of upper extremity actions versus action alone in children with unilateral cerebral palsy. Neurorehabil. Neural Repair 27 (9), 808–815. https://doi.org/10.1177/1545968313497101.
Sgandurra, G., Biagi, L., Fogassi, L., Sicola, E., Ferrari, A., Guzzetta, A., Tosetti, M., Cioni, G., 2018. Reorganization of the action observation network and sensory-motor system in children with unilateral cerebral palsy: an fMRI study. Neural Plast. 2018 https://doi.org/10.1155/2018/6950547.
Sgandurra, G., Biagi, L., Fogassi, L., Ferrari, A., Sicola, E., Guzzetta, A., Tosetti, M., Cioni, G., 2020. Reorganization of action observation and sensory-motor networks after action observation therapy in children with congenital hemiplegia: A pilot study. Dev. Neurobiol. 80 (9–10), 351–360. https://doi.org/10.1002/dneu.22783.
Simon-Martinez, C., Jaspers, E., Mailleux, L., Ortibus, E., Klingels, K., Wenderoth, N., Feys, H., 2018. Corticospinal tract wiring and brain lesion characteristics in unilateral cerebral palsy: Determinants of upper limb motor and sensory function. Neural Plast. 2018 https://doi.org/10.1155/2018/2671613.
Smithers-Sheedy, H., Mcintyre, S., Gibson, C., Meehan, E., Scott, H., Goldsmith, S., Watson, L., Badawi, N., Walker, K., Novak, I., Blair, E., 2016. A special supplement: findings from the Australian Cerebral Palsy Register, birth years 1993 to 2006. Dev. Med. Child Neurol. 58 (Suppl 2), 5–10. https://doi.org/10.1111/DMCN.13026.
Staudt, M., 2007. (Re-)organization of the developing human brain following periventricular white matter lesions. Neurosci. Biobehav. Rev. 31 (8), 1150–1156. https://doi.org/10.1016/J.NEUBIOREV.2007.05.005.
Staudt, M., Grodd, W., Gerloff, C., Erb, M., Stitz, J., Krägeloh-Mann, I., 2002. Two types of ipsilateral reorganization in congenital hemiparesis: A TMS and fMRI study. Brain 125 (10), 2222–2237. https://doi.org/10.1093/brain/awf227.
Staudt, M., Gerloff, C., Grodd, W., Holthausen, H., Niemann, G., Krägeloh-Mann, I., 2004. Reorganization in congenital hemiparesis acquired at different gestational ages. Ann. Neurol. 56 (6), 854–863. https://doi.org/10.1002/ana.20297.
Tinelli, F., Guzzetta, A., Purpura, G., Pasquariello, R., Cioni, G., Fiori, S., 2020. Structural brain damage and visual disorders in children with cerebral palsy due to periventricular leukomalacia. NeuroImage. Clinical 28. https://doi.org/10.1016/J.NICL.2020.102430.
Uryu, K., MacKenzie, L., Chesselet, M.F., 2001. Ultrastructural evidence for differential axonal sprouting in the striatum after thermocoagulatory and aspiration lesions of the cerebral cortex in adult rats. Neuroscience 105 (2), 307–316. https://doi.org/10.1016/S0306-4522(01)00203-2.
Verzelloni, J., Errante, A., Beccani, L., Filippi, M., Bressi, B., Cavuto, S., Ziccarelli, S., Bozzetti, F., Costi, S., Pineschi, E., Fogassi, L., Ferrari, A., 2021. Can a pathological model improve the abilities of the paretic hand in hemiplegic children? The PAM-AOT study protocol of a randomised controlled trial. BMJ Open 11 (12), e053910.
Wang, Y., Wang, H., Yu, Y., Xu, L., Chen, Y., Wu, D., 2015. [A voxel-based morphometric study on change of gray matter structures in cerebral palsy]. Zhonghua Er Ke Za Zhi = Chinese J. Pediatr. 53 (9), 696–700. https://europepmc.org/article/med/26757971.
Weinstein, M., Green, D., Geva, R., Schertz, M., Fattal-Valevski, A., Artzi, M., Myers, V., Shiran, S., Gordon, A.M., Gross-Tsur, V., Bashat, D.B., 2014. Interhemispheric and intrahemispheric connectivity and manual skills in children with unilateral cerebral palsy. Brain Struct. Funct. 219 (3), 1025–1040. https://doi.org/10.1007/S00429-013-0551-5.
Weinstein, M., Green, D., Rudisch, J., Zielinski, I.M., Benthem-Muñiz, M., Jongsma, M.L. A., McClelland, V., Steenbergen, B., Shiran, S., Ben Bashat, D., Barker, G.J., 2018. Understanding the relationship between brain and upper limb function in children with unilateral motor impairments: A multimodal approach. Eur. J. Paediatr. Neurol. 22 (1), 143–154. https://doi.org/10.1016/J.EJPN.2017.09.012.